

1           **Assessing potential impacts of shale gas development on shallow**  
2           **aquifers through upward fluid migration: A multi-disciplinary**  
3           **approach applied to the Utica Shale in Eastern Canada**

4  
5 Rivard, C.<sup>1\*</sup>, Bordeleau, G.<sup>1</sup>, Lavoie, D.<sup>1</sup>, Lefebvre, R.<sup>2</sup>, Ladevèze, P.<sup>1,2</sup>, Duchesne, M.J.  
6 <sup>1</sup>, Séjourné, S.<sup>3</sup>, Crow, H.<sup>4</sup>, Pinet, N.<sup>1</sup>, Brake, V.<sup>1</sup>, Bouchedda, A.<sup>2</sup>, Gloaguen, E.<sup>2</sup>, Ahad,  
7 J.M.E.<sup>1</sup>, Malet, X.<sup>1</sup>, Aznar, J.C.<sup>2</sup>, Malo, M.<sup>2</sup>

8  
9 <sup>1</sup> *Geological Survey of Canada, Natural Resources Canada, 490 rue de la Couronne, Québec,*  
10 *Québec, G1K 9A9, Canada*

11 <sup>2</sup> *Institut national de la recherche scientifique – Centre Eau Terre Environnement, 490 rue de la*  
12 *Couronne, Québec, Québec, G1K 9A9, Canada*

13 <sup>3</sup> *Enki GéoSolutions Inc., Montréal, Québec, H2V 4K7, Canada*

14 <sup>4</sup> *Geological Survey of Canada, Natural Resources Canada, 601 Booth Street, Ottawa, Ontario,*  
15 *K1A 0E8, Canada*

16  
17 *\* Correspond author: [christine.rivard@canada.ca](mailto:christine.rivard@canada.ca)*  
18  
19  
20

21 **Abstract**

22 Potential impacts of shale gas development on shallow aquifers has raised concerns,  
23 especially regarding groundwater contamination. The intermediate zone separating  
24 shallow aquifers from shale gas reservoirs plays a critical role in aquifer vulnerability to  
25 fluid upflow, but the assessment of such vulnerability is challenging due to the general  
26 paucity of data in this intermediate zone. The ultimate goal of the project reported here was  
27 to develop a holistic multi-geoscience methodology to assess potential impacts of  
28 unconventional hydrocarbon development on fresh-water aquifers related to upward  
29 migration through natural pathways. The study area is located in the St. Lawrence  
30 Lowlands (southern Quebec, Canada), where limited oil and gas exploration and no shale  
31 gas production have taken place. A large set of data was collected over a ~500 km<sup>2</sup> area  
32 near a horizontal shale gas exploration well completed and fracked into the Utica Shale at  
33 a depth of ≈2 km. To investigate the intermediate zone integrity, this project integrated  
34 research results from multiple sources in order to obtain a better understanding of the  
35 system hydrodynamics, including geology, hydrogeology, deep and shallow geophysics,  
36 soil, rock and groundwater geochemistry, and geomechanics. The combined interpretation  
37 of the multi-disciplinary dataset demonstrates that there is no evidence of, and a very  
38 limited potential for, upward fluid migration from the Utica Shale reservoir to the shallow  
39 aquifer. Microbial and thermogenic methane in groundwater of this region appear to come  
40 from the shallow, organic-rich, fractured sedimentary rocks making up the regional aquifer.  
41 Nonetheless, diluted brines present in a few shallow wells close to and downstream of a  
42 normal fault revealed that some upward groundwater migration occurs, but only over a few  
43 hundred meters from the surface based on the isotopic signature of methane. The

44 methodology developed should help support regulations related to shale gas development  
45 aiming to protect groundwater.

46 **Keywords:** shale gas, intermediate zone, aquifer vulnerability, upward fluid migration

47

## 48 **1 Introduction**

49

### 50 **1.1 Context**

51

52 The current pace of economic development is placing increasing demands on the  
53 exploitation of natural resources such as unconventional hydrocarbons, minerals and  
54 geothermal energy. These deep subsurface industrial activities are complex and may have  
55 significant environmental impacts, notably on freshwater aquifers used for water supply.  
56 So far, shallow aquifer vulnerability related to activities carried out at great depths  
57 (including hydraulic fracturing) has been the object of a limited number of studies, mainly  
58 because 1) the possibility of upward fluid migration through natural preferential pathways  
59 is perceived by some as being highly improbable and is still the object of an ongoing  
60 scientific debate (Vengosh et al., 2014; Birdsell et al., 2015; Lefebvre, 2017) and 2) very  
61 little information is available on the intermediate zone, located below shallow aquifers and  
62 above the zone targeted by the hydrocarbon industry (see Figure 1). It is, however,  
63 generally accepted that a natural connection between shallow and deep formations may be  
64 possible if large-scale permeable discontinuities (such as fault zones) are present across

65 this intermediate zone, constituting preferential migration pathways (Gassiat et al., 2013;  
66 Kissinger et al., 2013; Vengosh et al., 2014; Raynauld et al., 2016; Lefebvre, 2017). The  
67 expression of vertical fluid migration is difficult to directly visualize in continental settings.  
68 However, in marine environments, pockmarks and venting hydrocarbons in the water  
69 column are commonly observed and represent useful indicators of active upward fluid  
70 migration (Pinet et al., 2008).

71 One of the major societal concerns regarding the development of deep-seated  
72 unconventional oil and gas is the risk of shallow groundwater contamination due to upward  
73 migration of post-fracturing flowback fluids and hydrocarbons from deep geological  
74 formations (Vengosh et al., 2014; Vidic et al., 2013; BAPE 2014; CCA 2014; EPA 2016).  
75 This concern is even stronger in regions where aquifers represent the main water supply  
76 and where hydrocarbon development has not yet taken place (Raynauld et al., 2016). As a  
77 result, these perceived environmental issues have sometimes led to moratoria on hydraulic  
78 fracturing, such as in eastern Canada and northeastern USA, while in other areas (mostly  
79 where oil and gas production has been on-going for decades), concerns and regulatory  
80 efforts focussed on how to minimize or mitigate impacts (Esterhuysen, 2017).

81 A number of studies have been conducted to examine the potential for fluid migration from  
82 deep unconventional reservoirs to surficial freshwater aquifers. Although leakage from  
83 faulty casings appears to be the main mechanism by which gas could migrate from depth  
84 (Dusseault and Jackson; 2014; Nowamooz et al., 2014; Soeder et al., 2014; Ryan et al.,  
85 2015; Sherwood et al., 2016; Lefebvre, 2017), several authors have stressed the need for a  
86 better understanding and representation of potential preferential flow pathways (Gassiat et  
87 al., 2013; Kissinger et al., 2013; Birdsell et al., 2015; Reagan et al., 2015; Grasby et al.,

88 2016; Raynauld et al., 2016). Most of these studies have assessed the processes and  
89 conditions that could lead to upward fluid migration using numerical modelling based on  
90 generic conditions that may not represent the specific context of a given area.

91 On the other hand, many studies looking for indications of impacts on shallow aquifers  
92 have relied almost exclusively on geology and groundwater geochemistry and isotopes  
93 (e.g., Osborn et al., 2011; Warner et al., 2012; Jackson et al., 2013a; Molofsky et al., 2013;  
94 Darrah et al., 2014; McIntosh et al., 2014; McMahon et al., 2014; Moritz et al., 2015; Siegel  
95 et al., 2015; Humez et al., 2016; Nicot et al., 2017a, 2017b & 2017c). Early studies had  
96 suggested a link between groundwater quality and the distance to shale gas wells (Osborn  
97 et al., 2011; Jackson et al., 2013a), which had led to a scientific debate about the occurrence  
98 or not of such groundwater degradation. More recent studies in regions with or without  
99 shale gas exploitation have concluded that hydraulic fracturing and shale gas exploitation  
100 cannot be directly related to groundwater quality degradation (Siegel et al., 2015; Humez  
101 et al., 2016; LeDoux et al., 2016; Sherwood et al., 2016; Harkness et al., 2017; McMahon  
102 et al., 2017; Nicot et al., 2017a, 2017b & 2017c). Harkness et al. (2017) have stressed that  
103 controversies related to the potential for contamination from hydraulic fracturing have  
104 likely stemmed in large part from the lack of predrilling datasets (including a  
105 comprehensive suite of geochemical tracers), emphasizing the need to develop an  
106 understanding of the critical factors controlling the presence of elevated levels of  
107 hydrocarbon gas and salts in many aquifers located above shale gas reservoirs. McMahon  
108 et al. (2017) also warned that shale gas exploitation is a recent activity compared to the  
109 long residence time of groundwater, which may imply that today's absence of detectable  
110 impact does not mean that no impact would be observed in the long term.

111 While organic and inorganic groundwater geochemistry (including isotopes) represents a  
112 powerful tool, it relies on phenomena that are already happening and cannot be used only  
113 by themselves to fully understand, predict or eventually avoid potential contaminations  
114 from deep units. Therefore, groundwater geochemistry and isotopes should be  
115 complemented with other direct and indirect data to obtain a better knowledge and  
116 understanding of the intermediate zone, including its fracturing, its hydrogeological  
117 properties, its ability to transfer fluids and thus, its integrity. Industry-driven rock  
118 geochemistry, geomechanical and geophysical characterization have almost exclusively  
119 focussed on the deep hydrocarbon reservoir in an attempt to characterize and improve  
120 hydrocarbon recovery, thereby largely ignoring the intermediate zone. The need for  
121 research on the role of natural fractures and faults as pathways for methane and other fluids  
122 to reach shallow aquifers has been stressed by Ryan et al. (2015).

123 In spite of a significant recent increase in research on potential impacts of deep resource  
124 exploitation to shallow groundwater quality, there is currently no scientific consensus on  
125 how to assess these impacts based on the specific context of a basin or shale gas  
126 exploitation area. This highlights the importance of collecting scientific data to increase  
127 knowledge, inform debates and provide tools to help regulators protect and manage  
128 groundwater resources in areas where unconventional hydrocarbon resources are exploited.

129 In an effort in this regard, a holistic integrated study aiming to assess potential impacts of  
130 shale gas activities on shallow aquifers in the St. Lawrence Lowlands (southern Quebec,  
131 Canada) was initiated in 2012. This region only experienced limited exploration activities  
132 with no commercial production. The purpose of this study was to investigate a 500 km<sup>2</sup>  
133 area and evaluate whether its geological context presents a risk of aquifer contamination

134 prior to any potential large-scale drilling and fracturing activities. It was deemed critical to  
135 assess aquifer vulnerability to fluid upflow related to deep subsurface unconventional  
136 hydrocarbon exploitation in this frontier play, because groundwater is the local major  
137 source of water supply and strong societal protests against hydraulic fracturing had  
138 occurred. Since few data were available on the intermediate zone, in addition to  
139 conventional geological data our approach for this project involved the use of multi-source  
140 indirect data from different disciplines such as geophysics, geomechanics, hydrogeology,  
141 and rock and groundwater geochemistry. Extensive fieldwork was carried out including  
142 shallow well drilling (30 to 150 m deep), sampling of groundwater, soil, core and drill  
143 cuttings, shallow seismic surveys, borehole logging in shallow wells, airborne  
144 electromagnetic survey, structural surveys, hydraulic tests in sediments and bedrock, and  
145 groundwater monitoring. Multiple electric logs from shale gas wells as well as deep seismic  
146 profiles were also re-evaluated.

147 This paper presents an overview of the entire project and shows how diverse data types  
148 were integrated to assess the potential for fluid upflow from the unconventional shale gas  
149 reservoir. Sections 3 to 6 of this paper thus present an overview of the work carried out in  
150 each discipline, including its objective, fieldwork, methods used to interpret the acquired  
151 data and main results. Readers are referred to peer-reviewed papers on these specific  
152 studies to obtain more details. The understanding of the system hydrodynamics gained  
153 from the integration of results is discussed in section 7. A synthesis of other work that did  
154 not lead to useful results is provided in the Supplementary information.

155 The anticipated outcomes of this work were two-fold: 1) assess potential impacts of shale  
156 gas development on shallow aquifers through the identification of possible natural

157 connections between deep and shallow geologic formations in the Saint-Édouard study  
158 area and 2) contribute to the development of a methodology that could be used to assess  
159 aquifer vulnerability relative to deep subsurface activities, which could serve as a basis for  
160 regulatory frameworks aiming to minimize the potential impacts to aquifers. To our  
161 knowledge, this is the first time that such an aquifer vulnerability assessment is made on  
162 the basis of specific local and regional conditions.

163

## 164 **1.2 Description of the study area**

165

166 The study area is located in the St. Lawrence Lowlands in southern Quebec (Canada), in  
167 the Saint-Édouard region, on the south shore of the St. Lawrence River, about 65 km  
168 southwest of Quebec City (Figures 2 and 3). The study area overlies the Upper Ordovician  
169 Utica Shale, which was explored from 2007 to 2010 to assess its potential for shale gas  
170 production. Talisman Energy (now Repsol Oil & Gas Canada Inc.) drilled two wells in this  
171 area: one vertical, A267, and one horizontal, A275 (Figure 3). The horizontal well was the  
172 most promising one drilled in the Utica Shale in southern Quebec with post-fracking initial  
173 gas production of 340 000 m<sup>3</sup>/day (12 Mcf/d), which stabilized to 170 000 m<sup>3</sup>/day (6  
174 Mcf/d) after 25 days (Thériault, 2012).

175 The Utica Shale is part of the St. Lawrence Platform and extends over more than 10 000  
176 km<sup>2</sup> (Figure 2). Only 28 shale gas exploration wells were drilled over this vast area, of  
177 which 18 were hydraulically fractured, before the *de facto* shale gas exploration  
178 moratorium came into force in 2010 (Lavoie et al., 2014). Due to this limited number of

179 wells, the Utica Shale is considered a frontier play and, therefore, the St. Lawrence  
180 Platform is generally viewed as a “virgin” area with respect to hydraulic fracturing.

181 The topography of the ~500 km<sup>2</sup> study area shown on Figure 3 is relatively flat, having an  
182 elevation of nearly 90 m at the foot of the Appalachian piedmont, where well F2 was drilled  
183 (1.5 km south of the Talisman A267 and A275 wells), to ~30 m close to the St. Lawrence  
184 River. A ~20 m escarpment borders the south shore of the St. Lawrence River. Mean  
185 monthly temperatures vary between -11°C (in January) and 19°C (in July). Annual total  
186 precipitation is ~1170 mm, with about 23% falling as snow. Most residential wells in this  
187 area are open holes in the naturally fractured sedimentary rocks and have a steel casing  
188 across surficial sediments. Well depths vary from 20 to 80 m (average of ~50 m) and the  
189 wells are either under confined or semi-conditions (Ladevèze et al., 2016; Ladevèze, 2017),  
190 which allow them to be better protected against potential contamination from the surface  
191 (such as spills) than unconfined aquifers. The water table is relatively shallow in these low-  
192 permeability shales, ranging from 8.5 m deep to flowing artesian. The piezometric map  
193 (Ladevèze et al., 2016) shows that groundwater generally follows the topography, flowing  
194 from the Appalachians towards the St. Lawrence River.

195

## 196 **2 Geological context**

197

### 198 **2.1 Regional geological context**

199

200 In southern Quebec, a Cambrian – Ordovician sedimentary succession is preserved in the  
201 St. Lawrence Platform (Fig. 2) The succession records the evolution of the rift to passive  
202 margin and the final foreland basin events developed at the southern margin of the  
203 Paleozoic Laurentia craton (Lavoie, 2008; Lavoie et al., 2012).

204 In the upper 2 km depth of the study area, black organic-rich mudstones (Utica Shale and  
205 Sainte-Rosalie Group) are capped by shallowing-upward flysch (Lorraine Group) (Lavoie,  
206 2008). The Utica Shale is dominated by calcareous black shales with minor siltstone and  
207 is overpressured (BAPE 2010; Chatellier et al., 2013).

208 The St. Lawrence Platform strata are sub-horizontal and locally affected by mesoscopic  
209 open folds. High-angle generally SE-dipping normal faults displace in a staircase fashion  
210 the Precambrian basement and the St. Lawrence platform succession up to the Utica Shale  
211 with increased thickness of the sedimentary package on the downthrown fault block  
212 (Castonguay et al., 2010; Séjourné et al., 2013) (Fig. 2). These faults are exposed along the  
213 NW edge of the St. Lawrence platform (Fig. 3) and extend to the SE below the Appalachian  
214 tectonic wedge. Previous geological interpretations (Konstantinovskaya et al., 2009;  
215 Castonguay et al., 2010) suggested that normal faults do not extend in flysch and molasse  
216 units (Lorraine, Sainte-Rosalie and Queenston groups). The St. Lawrence Platform is  
217 bounded to the southeast by a deformed zone where Middle to Upper Ordovician platform  
218 units are imbricated in several compressive thrust panels; this zone is known as the  
219 parautochthonous domain (St-Julien et al., 1983; Castonguay et al., 2010). The Aston Fault  
220 marks the contact between the largely undeformed autochthonous St. Lawrence Platform  
221 and the parautochthonous domain (Figs. 2 and 3). The contact of the parautochthonous  
222 domain with the Appalachians corresponds to a regional low-angle thrust fault known as

223 the Logan's Line, which marks the position of the westernmost reach of allochthonous  
224 units (St-Julien et al., 1983; Castonguay et al., 2010) (Figs. 2 and 3). East of the Logan's  
225 Line, Paleozoic rocks of the Appalachians are steeply-dipping and involved in overturned  
226 NW-verging folds (Clark and Globensky, 1973).

227

## 228 **2.2 Saint-Edouard geological setting**

229

230 Surficial sediments in the Saint-Édouard area are usually thin (< 10 m) and made up of  
231 reworked tills and near-shore sediments of the former Champlain Sea, except in a few areas  
232 where fine-grained marine sediments have accumulated in local lows of the paleo-  
233 topography (Légaré-Couture et al., 2018; Rivard et al., 2018a).

234 Outcrops are sparse in this region, with the best sections exposed along the cliff on the  
235 shore of the St. Lawrence River and along small creeks (Clark and Globensky, 1973). The  
236 surface geology of the area consists of Upper Ordovician clastic-dominated units of the  
237 Lorraine Group (Nicolet and Pontgravé formations) and of the Sainte-Rosalie Group  
238 (Lotbinière and Les Fonds formations) (Fig. 3). The Lotbinière, Nicolet and Pontgravé  
239 formations are part of the St. Lawrence Platform (Fig. 3), whereas the Les Fonds Formation  
240 belongs to the parautochthonous domain (Fig. 3). The Lotbinière, Les Fonds and Nicolet  
241 formations consist of more or less calcareous mudstone and siltstone; these three units  
242 display variable content of organic matter and were shown to be in the oil window (Lavoie  
243 et al., 2016).

244 The area is characterized by several regional faults, which could hypothetically act as  
245 potential natural or enhanced migration pathways for deep fluids. The St. Lawrence  
246 Platform is cut by the Rivière Jacques-Cartier (RJC) normal fault system (Fig. 3), which  
247 limits the Lotbinière Formation to the southeast. The RJC fault is a lateral equivalent of the  
248 major Yamaska Fault (Fig. 2) and has significant vertical throw (see below). The Aston  
249 and Logan NW-verging thrust faults in the southeastern part of the study area limit the  
250 parautochthonous domain where the Les Fonds Formation is present. Between the RJC and  
251 Aston faults, the Upper Ordovician succession consists of the Nicolet Formation (Fig. 3).

252 The Upper Ordovician Utica Shale is considered hosting a significant volume of  
253 hydrocarbons (Dietrich et al., 2011; Chen et al., 2014 & 2017). Based on seismic (Lavoie  
254 et al., 2016) and hydrocarbon exploration well data (Thériault, 2012), the Utica Shale is  
255 present at variable depths in the study area: it was intercepted by wells at relatively shallow  
256 depths in the northern part of the area (271 m to 580 m) and at greater depths in the southern  
257 part (1857 m in the Saint-Édouard Talisman well). In all the wells, the Utica Shale is either  
258 stratigraphically overlain by the Nicolet Formation or structurally overlain by the Les  
259 Fonds Formation. The characteristics of each formation is provided in Lavoie et al. (2016).

260

### 261 **3 Seismic reflection**

262

263 *Objective*

264 2-D seismic surveys were used to investigate whether faults in the Saint-Édouard region  
265 reach the surface or not, as the latter could form primary control on fluid migration  
266 pathways and may act as hydraulic conduits connecting the shallow and deep subsurface  
267 (Caine et al., 1996; Faulkner et al., 2010; Bense et al., 2013). Seismic data consisted in one  
268 set of industry data originally collected in the early 1970s and reprocessed by Talisman  
269 Energy during the late 2000s, and two sets of near-surface data collected specifically for  
270 this project. The three seismic data sets aimed at being complementary by providing  
271 seismic images with different vertical resolutions of various depth intervals from the  
272 unconventional reservoir up to the surface.

273 In-house reprocessing of the industry data aimed at enhancing the resolution of the upper  
274 ~2 km bedrock reflections. However, acquisition parameters for the industry survey were  
275 set to image targets approximately located 1800 to 2800 m below the surface. Therefore,  
276 the first ~500 m were poorly imaged and difficult to interpret. New shallow seismic surveys  
277 were carried out to obtain key information on the near surface extensions of faults to  
278 complement the available industry survey. Acquired seismic lines thus included areas of  
279 the moderately dipping Logan's Line and Aston thrust fault, and the steeply dipping RJC  
280 normal fault (Figures 2 and 3). At the regional scale, these structural features are relatively  
281 well documented in the deep subsurface (Konstantinovskaya et al., 2009; Castonguay et  
282 al., 2010; Thériault, 2012), but their potential near-surface extension remains equivocal in  
283 the Saint-Édouard area. Shallow seismic surveys also aimed to help in positioning  
284 observation wells in or near faulted zones, so as to compare the permeability and  
285 groundwater quality of these zones with those of surrounding areas.

286 *Fieldwork and methods*

287 Shallow seismic surveys were performed using two types of vibrating sources: the Minivib  
288 (20-310 Hz) typically used for groundwater studies in unconsolidated sediments and the  
289 Envirovib (20-110 Hz) tentatively used in this project to fill the imaging gap between 50  
290 and 500 m. The Minivib was operated in the horizontal inline-mode (H1) and P and S  
291 arrivals were recorded using a 37.5 m long landstreamer equipped with 48 3-Component  
292 stations with a 0.75-m spacing (Pugin et al., 2009). The Envirovib was operated in vertical-  
293 mode and P-arrivals were recorded using one 480 m-long landstreamer including 96  
294 vertical-component stations with a 5-m spacing. In the Saint-Édouard area, a total of 18  
295 km and 15 km of shallow seismic data were collected respectively with Minivib and the  
296 Envirovib in 2013 and 2014.

### 297 *Results*

298 Results from the shallow seismic surveys were heavily impacted by the high velocity  
299 contrasts between the free surface (P-wave velocity of 300 m/s) or the thin Quaternary  
300 cover (P-wave velocity of 800 to 1700 m/s) and Paleozoic rocks (St. Lawrence Lowlands  
301 and Appalachians; P-wave velocity of 3800 to 4200 m/s). This high velocity contrast  
302 located at or almost at the free surface converts most of the seismic energy into surface  
303 waves, impairing shallow bedrock reflection imaging from low energy and high-frequency  
304 seismic sources. Despite these difficult geological conditions for seismic acquisition, the  
305 contact between the thin veneer of unconsolidated sediments and the bedrock was  
306 adequately imaged with the Minivib using P and S-waves recorded on the vertical and H1  
307 components of the station. All data parametrization attempts and filtering processes did not  
308 allow the Envirovib survey to be interpreted with confidence as this source simply lacked  
309 the energy to go beyond the strong velocity contrast that characterizes the first interface.

310 Therefore, given the specific near surface geological conditions, the shallow seismic  
311 surveys failed to locate the surface extension of faults imaged by the deep seismic survey.

312 A new subsurface interpretation of the area, below ~500 m, was made possible through the  
313 reprocessing of the industry deep seismic profile (Fig. 4a). The end-product confirmed the  
314 overall architecture of the Paleozoic successions and imaged the geometry of the St.  
315 Lawrence Platform and parautochthonous domain in greater details compared to most  
316 publicly-available vintage seismic lines (Lavoie et al., 2016). Several fault splays  
317 belonging to the RJC fault zone could be traced with confidence, some of which possibly  
318 extending to the near surface. These faults could represent potential fluid migration  
319 pathways, as shown by red arrows in Figure 4b. The geometry of the Appalachians SE of  
320 the Logan's Line remains poorly resolved by seismic data, due to structural complexity  
321 (Lavoie et al., 2016).

322

323 Based on the interpretation of the deep seismic (and due to a lack of good-quality data from  
324 the shallow seismic surface), four observation wells were drilled and five residential wells  
325 were sampled on both sides of the mapped normal fault potentially extending to the surface  
326 to obtain hydrogeological and geochemical information (see sections 5 and 6).

327

## 328 **4 Geomechanics**

329 *Objective*

330 A geomechanical study was carried out using petrophysical wireline logs from shale gas  
331 exploration wells in the Saint-Édouard area. The objective was to estimate geomechanical  
332 properties for the Utica Shale and the overlying intermediate zone, so as to identify the  
333 presence or absence of barriers to the propagation of hydraulic fractures towards the  
334 surface. To calibrate these values, laboratory geomechanical tests of core samples from the  
335 Lorraine Group and Utica Shale from the shale gas well had been planned. Unfortunately,  
336 these laboratory tests did not provide reliable results. Therefore, they are only briefly  
337 described in the Supplementary information section and discussed in Séjourné (2016).

### 338 *Data and Methods*

339 Publically available LAS digital files were integrated into the software Petra®, while DLIS  
340 files provided by Talisman Energy, containing all recorded data during logging campaigns,  
341 were used to verify the integrity and comprehensiveness of the LAS files and to  
342 occasionally complement them. Available data included gamma ray, caliper, density  
343 porosity, neutron porosity, resistivity curves, photoelectric factor, P and S waves, as well  
344 as bulk density and its correction curve. For a few wells, spectral gamma ray and  
345 mineralogy logs were also available.

346 Three shale gas exploration wells in or close to the study area had a complete borehole  
347 logging dataset and were thus used for this work: Saint-Édouard, Leclercville and  
348 Fortierville (Séjourné, 2016 & 2017). Acoustic logs (P and S waves) were used to derive  
349 elastic properties such as Poisson's ratios and Young's modulus. An acoustic brittleness  
350 index was derived from these two properties and a mineralogical brittleness index was  
351 derived from the mineralogy logs to better understand the observed variations between the

352 Utica Shale and its sedimentary cover. Subsequently, five additional conventional  
353 hydrocarbon exploration wells (drilled between 1972 and 1979) for which S-waves were  
354 not available were also used to extend the spatial coverage (Séjourné, 2017). To this  
355 purpose, a synthetic S-wave was generated for these wells and synthetic elastic modules  
356 were then calculated, allowing the estimation of the geomechanical properties.

### 357 *Results*

358 Values for Young's modulus and Poisson's ratios show that a large mechanical contrast  
359 exists between the brittle calcareous Utica Shale and more ductile clayey shales of the  
360 Lorraine Group. This relationship is best exemplified by the brittleness indexes shown in  
361 Figure 5, where a sharp contrast is observed at the contact between the upper part of the  
362 Utica Shale and the base of the Lorraine Group. Figure 5 also illustrates the good agreement  
363 between results obtained from acoustic and mineralogy logs. During hydraulic fracturing,  
364 the propagation of induced fractures within the more brittle Utica Shale would be severely  
365 limited or even stopped by these overlying ductile units. The geomechanical study thus  
366 strongly suggests that units of the intermediate zone (Lorraine Group) represent an efficient  
367 barrier to the propagation of hydraulic fractures, thus providing a good protection for the  
368 shallow groundwater aquifers. Nonetheless, these geomechanical property values remain  
369 indicative and qualitative, and should be taken with caution in absence of calibration with  
370 laboratory tests (see the Supplementary information section and Séjourné, 2017).

371

## 372 **5 Hydrogeology**

373

374 Hydrogeological fieldwork included the drilling of 15 observation wells, borehole logging  
375 of these wells, hydraulic tests in wells and permeability tests in surficial deposits.

376

### 377 **5.1 Well drilling**

#### 378 *Objective*

379 Drilling of 15 observation wells into the regional fractured rock aquifer provided cuttings  
380 or core samples and groundwater samples in key locations. These wells provided  
381 information about stratigraphy, hydraulic conductivity and natural fractures. Locations of  
382 observation wells were strategically chosen to gain information, first on specific areas to  
383 improve spatial and formation coverage and second in the vicinity of mapped fault zones,  
384 whose positions are uncertain.

#### 385 *Fieldwork*

386 Of the fifteen observation wells that were drilled, seven were hammer drilled (F5, F6 and  
387 F10 to F14) and eight were diamond drilled (F1 to F4, F7, F8, F20 and F21). Characteristics  
388 of these wells are provided in Ladevèze et al. (2016) and Table S-1 of the Supplementary  
389 information and their location is shown in Figure 3. The diamond-drilled wells provided  
390 core samples for stratigraphic assessment and organic geochemistry. Observation wells  
391 have a depth range of 30 to 147 m and they are all open in bedrock. Each well was

392 instrumented with a datalogger to record water levels and. three of these wells were also  
393 equipped with barometers.

394

## 395 **5.2 Fracture characterization**

### 396 *Objective*

397 The main purposes of acquiring data on natural fractures were to characterize the geometry  
398 of the fracture network affecting the sedimentary succession in the Saint-Édouard region  
399 and to assess the continuity of structural features from deep to shallow units. Information  
400 on fractures were derived from bedrock outcrops, shallow observation wells through  
401 borehole geophysical logging, and three shale gas exploration wells using Formation Micro  
402 Imager (FMI) logs for depths exceeding 560 m. Since this project aims to assess the  
403 potential for upward fluid migration from the shale gas reservoir to surficial aquifers, the  
404 study of fracture networks was a key component.

### 405 *Fieldwork*

406 Shallow borehole logging was carried out in 11 observation wells. This work aimed to  
407 collect data on fractures (orientation, dip and aperture), bedrock lithology, compressional  
408 (P) and shear (S) wave velocities in the bedrock, fluid temperature and electrical  
409 conductivity, as well as identify zones of fracture flow. The suite of tools consisted of  
410 natural gamma-ray and guard resistivity, optical and acoustic televiewers, full waveform  
411 sonic logs, fluid temperature, fluid conductivity, and heat-pulse flowmeter. Since ambient  
412 flow (i.e. natural upward/downward gradients in borehole fluid) was not observed in any  
413 well, an impeller (Grundfos Redi-Flo 2) pump was used to induce upward flow in boreholes

414 for the heat pulse flowmeter testing. Data on fractures (orientation, density, spacing, cross-  
415 cutting relationships) were also collected from 15 bedrock outcrops, mainly located close  
416 to the St. Lawrence River (Ladevèze, 2017; Ladevèze et al., 2018a).

#### 417 *Methods*

418 Fractures identified using borehole geophysical logging were classified as open, closed or  
419 broken zones. Open and broken features were further classified as “flowing” based on flow  
420 indications. . P- and S-wave velocities were computed from full waveforms using a  
421 semblance processing routine to obtain slowness ( $\mu\text{s/m}$ ) of P and S waves, and calculate  
422 velocity logs (details are available in Crow and Ladevèze, 2015).

423 FMI images were used to examine fracture densities, fracture types (open or closed) and  
424 orientations. Estimates of apertures from these images were provided by Talisman Energy.  
425 Imaged vertical sections for the three shale gas wells varied from 560 m to 2320 m deep,  
426 but were mostly located in the lower part of the Lorraine Group and in the underlying Utica  
427 Shale and (below 1500 m). Images of horizontal sections for each shale gas well, drilled  
428 into the Utica Shale, over lengths varying from 920 to 1000 m, were also available.

429 Chronology of fractures was based on intersection relationships and through fold test in  
430 order to calculate the fracture attitudes prior to folding events. Fracture spacing was also  
431 estimated to characterize the spatial organization of these structures using variograms.

#### 432 *Results*

433 Four fracture sets were defined: three sub-vertical sets (FS1, FS2 and FS3) and one sub-  
434 horizontal, corresponding to bedding plane fractures (BPF). FS1 and FS2 are orthogonal

435 to each other and to the bedding planes. They can be found everywhere throughout the  
436 shallow and deep intervals, however in shale units they seem to be clustered in “corridors”,  
437 while in siltstone beds they are more uniformly spatially distributed. Fractures from FS3  
438 are more sparsely distributed and were mainly observed in the Utica Shale. BPF could only  
439 be observed at shallow depths, but are assumed to be present deeper, based on other studies  
440 examining shale successions (Gale et al., 2007; Gale et al., 2015; Wang and Gale, 2016).  
441 Based on the similarities between the shallow and deep fracture datasets and also based on  
442 the regional geologic and tectonic history, it was assumed that the fracture network  
443 characterization could also be applied to the intermediate zone (Ladevèze et al., 2018a).  
444 Figure 6 presents conceptual models of the fracture network for the entire sedimentary  
445 succession of the Saint-Édouard area.

446 Fracture data obtained from the shallow and deep intervals revealed that most fractures are  
447 open in the shallow rock aquifer, while very few fractures are open at depth. Most of these  
448 shallow fractures are present within the first 60 m of the rock, and especially the upper 30  
449 m (Ladevèze et al., 2018b). At depth, fractures from only one fracture set (FS1) were found  
450 to be quite commonly open in the shale gas reservoir (21% of all FS1 fractures), and thus,  
451 by extension, very likely in the intermediate zone. FMI images also showed that the  
452 calcareous and brittle Utica Shale is more densely fractured than the Lorraine Group units  
453 (Séjourné, 2017). Denser fracture networks were, however, observed in the close vicinity  
454 of some of the thrust faults, with fractures generally oriented in the same direction as the  
455 FS1 fracture set. Implications of their presence on groundwater flow are discussed in  
456 section 5.3.

457

### 458 **5.3 Hydraulic properties, groundwater flow and confinement conditions**

#### 459 *Objective*

460 Hydraulic conductivities ( $K$ ) of shallow and deep rock formations were estimated to better  
461 understand the system hydrodynamics and to define hydrogeological conditions, as well as  
462 the role of fractures in groundwater flow. For the shallow intervals,  $K$  values were acquired  
463 through *in situ* hydraulic tests and theoretical equations were used for the deep interval.  
464 The goal for the deep interval assessment was to propose a semi-quantitative estimate of  
465 hydraulic properties based on available data and to develop a conceptual model of the  
466 fracture network to make a preliminary assessment of potential upward fluid migration  
467 through these structural features.

#### 468 *Fieldwork*

469 *In situ* hydraulic tests were carried out in shallow observation wells using slug tests.  
470 However, the least permeable wells ( $10^{-8}$  m/s or less, see Table S-1 in Appendix) were  
471 instead pumped for a short period using a low-yield impeller pump (Grundfos Rediflo2) to  
472 avoid very large drawdowns that would have taken weeks to recover (see details in  
473 Ladevèze et al., 2016).

474 Water-level and barometric measurements were recorded every 15 minutes using pressure  
475 transducers (dataloggers). The purposes of acquiring these data series were 1) to help  
476 define confinement conditions and 2) to estimate aquifer recharge for wells under  
477 unconfined conditions.

#### 478 *Methods*

479 Hydraulic conductivities ( $K$ ) for the shallow observation wells were estimated from slug  
480 tests using two interpretation methods (Bouwer and Rice, 1976; Hyder et al., 1994). Both  
481 methods provided similar results. For the deep interval, hydraulic properties (porosity and  
482 hydraulic conductivity) were estimated based on fracture apertures, fracture spacing and  
483 density (see representative elementary volumes in Fig. 8) integrated in the cubic law  
484 assuming laminar flow between two parallel plates (Snow, 1968; Bear, 1993). Porosity was  
485 estimated as a percentage of the fracture volume in a quasi-impermeable matrix, based on  
486 available fracture characteristics and estimates of inter-cluster (or inter-corridor) distance.

#### 487 *Results*

488 Hydraulic conductivities ( $K$ ) of the shallow interval, which is the active groundwater flow  
489 zone (upper 60 m of the rock aquifer), range between  $2 \times 10^{-9}$  and  $1 \times 10^{-5}$  m/s. The  
490 geometrical mean is higher in the autochthonous domain ( $1.8 \times 10^{-6}$  m/s) than in the other  
491 two domains ( $2.3 \times 10^{-7}$  m/s). In addition, the range of values in the parautochthonous and  
492 allochthonous domains is wider than in the autochthonous domain. Restricted to the upper  
493 part of the Lorraine Group, siltstone beds are less than 10 cm thick and they are present in  
494 meter- to decameter-thick intervals; they are densely fractured (see Figure 6). Hydraulic  
495 tests have not indicated different permeabilities close to known (mapped) faults compared  
496 to those of the adjacent domain. Since open fractures in the shallow aquifer can locally  
497 display some large apertures, the fracture network significantly contributes to the total  
498 porosity of the rock mass (which is approximately 8%).

499 As very few fractures are open at depth and generally belong to a single set (FS1, see  
500 section 5.2), these fractures should not increase significantly the shale porosity and

501 permeability, and hence should not favour fluid circulation because the possibility for  
502 fracture interconnection is very limited. Moreover, clay-gouge was observed in cores of  
503 shale gas wells drilled in the thrust fault zone (Ladevèze, 2017); therefore, given the shale  
504 - siltstone dominated succession in the entire study area, the presence of clay-gouge in the  
505 undrilled normal fault zone is strongly suspected due to the presence of potential secondary  
506 inverse-compressive fault-anticlines suggested from the reprocessed seismic line over the  
507 trace of the RJC fault (Lavoie et al., 2016). Therefore, flow across fault zones is considered  
508 very unlikely in this region. Within the deep intervals (intermediate zone and Utica Shale),  
509 very low hydraulic conductivities ( $K$ ) in the order of  $10^{-12}$ - $10^{-18}$  m/s were estimated with  
510 the cubic law. These values are in agreement with values found in the literature for the  
511 Lorraine Group and Utica Shale (BAPE 2010; Séjourné et al., 2013).

512 While estimated hydraulic conductivities are very low, two features could possibly locally  
513 increase permeability in the two fault zones of the study area. In the thrust fault zone, open  
514 fractures were found to be more frequent in the damage zone surrounding the fault planes.  
515 However, they are also mainly in the same direction as fractures from FS1, hence limiting  
516 possible fracture interconnections. In the normal fault zone, siltstone beds, which are more  
517 permeable than shale strata and appear to be relatively frequent in the upper part of the  
518 Lorraine Group (Lavoie et al., 2016), were inferred to have been dragged into the core of  
519 the normal fault (Ladevèze, 2018b), an assumption based on data from abandoned (old)  
520 hydrocarbon exploration well logs, various geological descriptions and geochemical  
521 findings (see section 6.1). This possible increase in permeability could not, however, be  
522 quantified, as no hydraulic data are available at depth in this region. Pressure gradient data  
523 for the shallow intermediate zone is not available either, although it is well known that the

524 deeper Utica Shale is overpressured (Chatellier et al., 2013; Séjourné et al., 2013;  
525 Konstantinovskaya et al., 2009). Nevertheless, the possibility that these fault zones act as  
526 large-scale flow pathways seems extremely unlikely (Ladevèze et al., 2018b).

527

## 528 **6 Geochemistry**

529

530 The groundwater and rock geochemistry study mainly focussed on the characterization of  
531 hydrocarbons (concentration and isotopic composition) from observation wells. These  
532 results were compared to the organic geochemistry data from the deep Utica Shale.

533

### 534 **6.1 Groundwater geochemistry**

#### 535 *Objective*

536 As the main objective of the project was to investigate the potential for upward fluid  
537 migration from the shale gas reservoir to freshwater aquifers, it was crucial to sample and  
538 analyze shallow groundwater to see if it contained thermogenic gas and, if so, to determine  
539 its provenance. Isotopic geochemistry is a valuable tool to investigate the origin (microbial  
540 or thermogenic) of methane and its possible relation with the shale gas reservoir. Therefore,  
541 a multi-isotope approach was used, which included both stable and radioactive isotopes.

#### 542 *Fieldwork and analyses*

543 Groundwater was sampled from 14 of the 15 observation wells (well F14, located in the  
544 thrust fault zone and likely in gouge, remained dry throughout the duration of the project),  
545 as well as in 30 residential wells in order to obtain a better spatial coverage. Among the 44  
546 sampled wells, seven were sampled regularly over a period of up to 2.5 years at intervals  
547 between one to four months (see section 6.3). Groundwater was sampled at specific  
548 targeted depths in observation wells, where borehole geophysics had previously located  
549 flowing fractures.

550 Observation wells were sampled using a low-flow yield according to the EPA guidelines  
551 (Puls and Barcelona, 1996) using a submersible pump (either an impeller or a bladder  
552 pump), or HydraSleeve bags for the deepest well (F21). These sampling techniques  
553 provided similar results when tested systematically in 10 wells over three sampling  
554 campaigns (Rivard et al., 2018b). Residential wells were also sampled at a low yield from  
555 an outdoor tap, prior to any treatment. Samples for alkane concentrations and isotopic  
556 composition were collected under a head of water (method described in Bordeleau et al.,  
557 2018a, 2018b & 2018c), which minimizes degassing but does not prevent it completely  
558 when methane is effervescent (Molofsky et al., 2016). Hence, when downhole  
559 concentrations are above the methane saturation point at atmospheric pressure, measured  
560 concentrations are expected to be underestimated compared to true downhole  
561 concentrations.

562 Groundwater samples were collected and analysed for a wide variety of compounds  
563 including major and minor ions and trace metals, alkane concentrations ( $C_1$  to  $C_3$ ), VOCs,  
564 stable isotope composition of water ( $\delta^2H$  and  $\delta^{18}O$ ) and of methane, ethane and propane  
565 ( $C_1$  to  $C_3$ - $\delta^{13}C$  and  $-\delta^2H$ ; when concentrations allowed), dissolved inorganic carbon (DIC-

566  $\delta^{13}\text{C}$ ),  $^{222}\text{Rn}$ , tritium ( $^3\text{H}$ ), as well as radiocarbon ( $^{14}\text{C}$ ) in methane and DIC, and finally  
567  $^{36}\text{Cl}$ . Some of these analyses are quite atypical for this type of project (e.g.,  $^{36}\text{Cl}$ ,  $\text{CH}_4\text{-}^{14}\text{C}$ )  
568 and they provided important information on groundwater age and hydrocarbon source.  
569 Analytical methods used in the different laboratories are described in details in Bordeleau  
570 et al. (2018a, 2018b & 2018c).

## 571 *Results*

572 Groundwater, which is generally potable in the region (based on metal, anion and VOC  
573 results), was classified into four water types according to the dominant cation and anion(s)  
574 in the samples. They are, in order of geochemical evolution:  $\text{Ca-HCO}_3$ ,  $\text{Na-HCO}_3$ ,  $\text{Na-}$   
575  $\text{HCO}_3\text{-Cl}$  and  $\text{Na-Cl}$  (Figure 7). There is no particular pattern in the spatial distribution of  
576 water types in the study area; instead, transitions occur vertically, and hence the major ion  
577 geochemistry is mostly related to sampling depth. Chemical evolution first occurs through  
578 ion exchange with the aquifer matrix, and additional salinity is gained through mixing with  
579 residual water of the Late Quaternary Champlain Sea water, which invaded this area  
580 between 13,000 and 11,000 years ago (Occhietti and Richard, 2003). While the bulk of the  
581 water in all water types is consistent with a meteoric origin (based on  $\text{H}_2\text{O-}\delta^2\text{H}$  and  $-\delta^{18}\text{O}$   
582 values), the contribution of Champlain Sea residual water to salinity in the  $\text{Na-HCO}_3\text{-Cl}$   
583 and  $\text{Na-Cl}$  water types throughout the study area is confirmed by a chloride to bromide  
584 ( $\text{Cl/Br}$ ) molar ratio close to the seawater ratio of 639 (Hounslow, 1995). Another source of  
585 salinity that was identified in a few wells is formation brines, as even small amounts of  
586 these saline brines cause a high salinity in the samples, accompanied by a  $\text{Cl/Br}$  ratio well  
587 below that of seawater.

588 Samples with clear indication of deep formation brines were found to be located mainly  
589 close to (F5, F7, Zone 10R, Zone 11R2) or downstream (F1, F20, INRS-447) of the normal  
590 fault zone (Figure 7), suggesting that it acts as a discharge zone for deep regional  
591 groundwater flow (Bordeleau et al., 2018a, and section 7.1). Analyses of radioisotopes in  
592 samples from the bottom of wells F7 and F20 confirmed the very old apparent (bulk) age  
593 of this water, in the order of nearly 2 million years (based on  $^{36}\text{Cl}$  values), with no  
594 contribution (F7) or very little contribution (F20) of modern recharge (based on  $^3\text{H}$  and  
595  $\text{DIC-}^{14}\text{C}$  values). Groundwater radon analyses ( $^{222}\text{Rn}$ ) did not show any abnormally high  
596 values in the study area (the highest being 24 Bq/L), but the highest values were found  
597 close to the normal fault zone or downstream of it (Bordeleau et al., 2018c, and Figure S1  
598 of the Supplementary Information section).

599 Dissolved methane was found to be ubiquitous in the study area, being detected in 96% of  
600 the sampled wells. The median concentration for all visited wells was 4.9 mg/L, with values  
601 in individual samples ranging from below detection limit (<0.006 mg/L) to 82 mg/L  
602 (Bordeleau et al., 2018a). The large spatial variations cannot be explained by differences  
603 in bedrock geology (Figure 7), but are strongly correlated to the water type and by  
604 extension, to the sampling depth and groundwater age (Bordeleau et al., 2018a). Higher  
605 methane concentrations were found in Na-rich evolved water, an observation in agreement  
606 with many other studies (Molofsky et al., 2013 and 2016; Darrah et al., 2014; Moritz et al.,  
607 2015; LeDoux et al., 2016; Siegel et al., 2015). A few wells also had significant  
608 concentrations of ethane and propane, which is an indication of the presence of  
609 thermogenic gas, since microbes can only produce very small amounts of these two  
610 molecules (Tazaz et al., 2013).

611 The origin of the natural gas found in groundwater can be ascertained from various  
612 geochemical graphs. The commonly-used Bernard graph (Bernard et al., 1976) showing  
613 the dryness ratio ( $C_1/[C_2+C_3]$ ) versus methane carbon isotope values is presented in Figure  
614 8. All individual samples collected in all wells are represented; for those with no ethane  
615 and propane, a dryness ratio cannot be computed, but was assigned an arbitrary value of  
616 100 000 (at the top of the graphs, in the “unquantified ratios” box). Results from most  
617 samples fall outside of the traditional domains for microbial and thermogenic gas (Figure  
618 8-A). This could be due to mixing between microbial and thermogenic gas, or to  
619 biogeochemical processes affecting the isotopic composition of microbial gas.

620 Mixing with thermogenic gas was confirmed in 15% of the wells, based on the presence of  
621 ethane and/or propane (Figure 8-B). These wells are not clustered in a specific area or  
622 located specifically along fault zones (Figure 7, see red circles). However, the only  
623 groundwater sample that falls within the ‘thermogenic’ domain on Figure 8 (shown with a  
624 red arrow), was collected in a well located along the RJC fault. The  $CH_4-\delta^{13}C$  value of this  
625 sample corresponds to deep formation gas from the Lorraine Group, but not to the Utica  
626 Shale (values published in Chatellier et al., 2013). This residential well was sampled  
627 several times afterward, but all subsequent samples contained only microbial gas.

628 For samples without ethane or propane, other processes must be invoked to explain  
629 ambiguous  $CH_4-\delta^{13}C$  values. The process that is most often suspected is oxidation, which  
630 causes an increase in both  $CH_4-\delta^{13}C$  and  $-\delta^2H$  values. Considering the  $CH_4-\delta^2H$  values in  
631 our samples, and based on published isotopic fractionation factors for methane oxidation,  
632 this process does not appear to be significant in the Saint-Édouard area, except for Ca-  
633  $HCO_3$  type samples with very low methane concentrations and relatively high  $CH_4-\delta^{13}C$

634 values (pink diamonds on Figure 8-A). Moreover, comparison of  $\text{CH}_4\text{-}\delta^2\text{H}$  and  $\text{H}_2\text{O-}\delta^2\text{H}$   
635 values confirmed that methane isotopic values in most samples are consistent with regular  
636 (non-oxidized) microbial methane formed via the  $\text{CO}_2$  reduction pathway using the local  
637 groundwater (Bordeleau et al., 2018b).

638 Another process that may explain ambiguous isotopic values is late-stage methanogenesis,  
639 which is the result of kinetic isotope effects occurring during microbial transformation of  
640 substrates (mostly  $\text{CO}_2$  in this region) into methane, in an isolated groundwater reservoir  
641 where the carbon (reactant) pool has substantially been used up and is not replenished by  
642 fresh DIC from active recharge (Whiticar et al., 1999). Gas produced through this process  
643 is characterized by high dryness ratios typical of microbial methane, relatively high  $\text{CH}_4\text{-}$   
644  $\delta^{13}\text{C}$  values resembling thermogenic gas, and higher than expected  $\text{DIC-}\delta^{13}\text{C}$  values. An  
645 in-depth interpretation of these geochemical parameters (Bordeleau et al., 2018b) revealed  
646 that many samples contained late-stage microbial gas (Figure 8-C). Noteworthy, several of  
647 these samples also contain some thermogenic gas (Figure 8-B, C). Analyses of methane  
648 radiocarbon ( $\text{CH}_4\text{-}^{14}\text{C}$ ), and comparison with  $\text{DIC-}^{14}\text{C}$  values in the aquifer, confirmed that  
649 the late-stage microbial gas was produced in the distant past ( $^{14}\text{C}$ -free), while the regular  
650 microbial produced at shallower depths in the aquifer tends to be more recent ( $^{14}\text{C}$ -bearing).

651 Finally, stable isotopic composition of ethane and propane, when available, did not provide  
652 additional information on the possibility of upward migration, as the values measured in  
653 groundwater, shallow bedrock gas and deep formation gas (Lorraine and Utica shales) span  
654 similar ranges (Bordeleau et al., 2018b).

655

656 **6.2 Rock geochemistry**

657 *Objective*

658 As 15% of the sampled wells contained dissolved thermogenic methane, it was necessary  
659 to determine the origin of that methane. If methane had been found to originate from the  
660 Utica Shale, it would have implied the presence of natural fluid migration pathways from  
661 the shale gas reservoir to the shallow groundwater. Therefore, initial organic geochemical  
662 analyses were carried out on shallow core samples to document gas characteristics in the  
663 upper 150 m, mainly composed of black shale units. The purpose of these analyses was  
664 mainly to provide the concentrations and isotopic ( $\delta^{13}\text{C}$  and  $\delta^2\text{H}$ ) compositions of alkanes  
665 ( $\text{C}_1\text{-C}_3$ ) that were shown to be present in shallow bedrock and compare these values to  
666 those of dissolved natural gas in groundwater.

667 *Fieldwork*

668 Drill cuttings and core samples were collected during the drilling campaigns. Both were  
669 stored in Isojars® (Isotech Laboratories, Champlain, IL) containing ultrapure water and a  
670 bactericide during the 2014 campaign. A triplicate of Isojars® were collected  
671 approximately every 10 to 15 m, leading to a total number of samples per well varying  
672 from 3 to 10. Gas composition was analysed for 39 samples. Some core samples were also  
673 preserved in a double-layer vacuum plastic bag for pore-water analyses and some were  
674 disinfected and stored in aluminium foil, then frozen, for phospholipid fatty acid (PLFA)  
675 analyses. Analyses of the last two types of samples did not provide the expected results;  
676 they are thus only briefly discussed in the Supplementary information section.

677 *Methods*

678 Drill cuttings and core samples preserved in the Isojar® were initially analysed by Rock-  
679 Eval to assess the presence of pore-space free and adsorbed hydrocarbons as well as their  
680 thermal maturation. The latter was also evaluated through organic petrography of the  
681 samples. Gas extracted from drill cuttings and core samples (accumulated in the Isojar®  
682 headspace) was analysed for both alkane concentrations and isotopic composition.  
683 Therefore, the complete set of analyses included: Rock-Eval pyrolysis, petrographic  
684 observation of organic matter reflectance, alkane concentrations ( $C_1$  to  $C_3$  or  $C_1$  to  $C_5$   
685 depending on the laboratory), alkane isotopic composition ( $C_1$  to  $C_3$ ) for  $\delta^{13}C$  and  
686 sometimes  $\delta^2H$  (depending on the laboratory), and  $^{14}C$  of methane. Methods used in  
687 laboratories for the different analyses are described in Lavoie et al. (2016) and Bordeleau  
688 et al. (2018b).

### 689 *Results*

690 All rock samples from the Les Fonds, Lotbinière and Nicolet formations showed organic  
691 matter typical of Type II kerogen, the three units are thermally mature and have reached  
692 oil window conditions at the time of maximum burial. The Lotbinière and Les Fonds  
693 formations have total organic carbon (TOC) content of a fair hydrocarbon source rock  
694 (TOC>0.5%), whereas the Nicolet Formation has a lower TOC content and is considered  
695 as a poor hydrocarbon source rock (Lavoie et al., 2016).

696 All shallow bedrock samples contained gas hydrocarbons, but with locally variable  
697 composition and concentration that were not always linked to specific bedrock units. Over  
698 the depth range covered by samples, a downward increase in the concentration of alkanes  
699 ( $C_1+C_2+C_3$ ) was observed, often along with a decrease in the gas dryness ratio ( $C_1/[C_2+C_3]$ )

700 (Lavoie et al., 2016). In fact, samples with dryness ratios  $<100$  (thermogenic gas) were  
701 found along the whole depth range, but samples with ratios between 100 and 1000 (mixed  
702 gas) were restricted to the top 50 m of bedrock. Likewise, samples with  $\text{CH}_4\text{-}\delta^{13}\text{C}$  values  
703 corresponding to thermogenic gas ( $>-50\text{‰}$ ) or mixed gas ( $-60$  to  $-50\text{‰}$ ) were found over  
704 the whole depth range, while samples with microbial values ( $<-60\text{‰}$ ) were generally  
705 restricted to the top 15 m of bedrock. This suggests that in the top part of the fractured rock  
706 aquifer, the thermogenic gas that was originally present in the bedrock pores has escaped  
707 and/or was affected by microbial degradation, while ongoing *in situ* methanogenesis in this  
708 active part of the aquifer adds microbial gas.

709 Isotopic results and dryness ratios for shallow bedrock samples appear on Figure 8 (grey  
710 diamonds), along with deep formation gas ( $>600$  m) from the Lorraine and Utica shales  
711 (black diamonds) published by Chatellier et al. (2013). The  $\text{CH}_4\text{-}\delta^{13}\text{C}$  ratios of shallow  
712 bedrock gas have limited overlap with those of the deep formation gas, which typically  
713 show isotopically-enriched values. The presence of unambiguously thermogenic gas in  
714 some shallow bedrock samples, and the mix of microbial and thermogenic gas in others, is  
715 confirmed by a Whiticar (1999) plot of  $\text{CH}_4\text{-}\delta^{13}\text{C}$  versus  $\text{CH}_4\text{-}\delta^2\text{H}$  values (see Lavoie et al.,  
716 2016). As mentioned in section 6.1, the  $\delta^{13}\text{C}$  values of  $\text{C}_2$  and  $\text{C}_3$  alkanes are  
717 indistinguishable from values for the deep formation gas samples (Lavoie et al., 2016).

718 The  $\text{CH}_4\text{-}\delta^{13}\text{C}$  ratios of shallow rock samples overlap with groundwater results for a large  
719 part, but more thermogenic gas was found in rock (Figure 8), confirming that thermogenic  
720 gas is trapped in rock pores, while recent microbial gas is constantly forming and dissolving  
721 in groundwater. A comparison of  $\text{CH}_4\text{-}\delta^{13}\text{C}$  and  $-\delta^2\text{H}$  values for shallow bedrock and  
722 groundwater was also made on a well by well basis, showing that values were very similar

723 for a given well and sampling depth (Bordeleau et al., 2018b). Based on these findings, the  
724 likely source of thermogenic gas in groundwater appears to be the shallow fractured rock  
725 aquifer itself (which is mainly composed of organic-rich black shale), rather than the deep  
726 Utica Shale (Lavoie et al., 2016).

727

### 728 **6.3 Groundwater monitoring**

#### 729 *Objective*

730 The objective of monitoring dissolved methane concentration and its isotopic composition  
731 was to document natural variations in wells with different characteristics. Knowledge of  
732 these temporal variations for a given area and even for a given well prior to any shale gas  
733 development is critical, mainly to distinguish natural fluctuations from anthropogenic  
734 impacts stemming from deep industrial activities. Until now, few studies have documented  
735 such variations (e.g.: Coleman and McElreath, 2012; Gorody, 2012; Humez et al., 2015;  
736 Sherwood et al., 2016; Smith et al., 2016; Currell et al., 2017, Botner et al., 2018) and they  
737 have relied on only a few wells and/or on a few sampling events.

#### 738 *Fieldwork and methods*

739 Monitoring was carried out over more than two years in six wells, including four  
740 observation wells (F1 to F4) and two residential wells (INRS-447 and Zone 9R). Well F21,  
741 which was drilled later in the project, was subsequently added to the monitoring program  
742 and was sampled over 15 months. The selected wells reflect the diversity of wells present  
743 in this study area (e.g.: high and low methane concentrations, observation and residential  
744 wells, shallower and deeper wells, purely microbial gas and mixed gas). Groundwater was

745 sampled for alkane (C<sub>1</sub>-C<sub>3</sub>) concentrations, methane isotopic composition (CH<sub>4</sub>-δ<sup>13</sup>C and  
746 -δ<sup>2</sup>H), and DIC-δ<sup>13</sup>C analyses. Groundwater sampling was carried out as described in  
747 section 6.1.

#### 748 *Results*

749 Results showed that dissolved methane concentrations can fluctuate greatly even in the  
750 absence of industrial activities, depending on the sources of gas and microbial activity.  
751 Some examples from monitoring wells are presented in Figure 9. For the Saint-Édouard  
752 area and for the monitored period, methane concentrations varied from 2.5 to 6 times the  
753 lowest recorded values for a given well (with sampling depth and sampling technique  
754 remaining the same), which is well above the uncertainty expected for sampling, handling  
755 and analysis (Rivard et al., 2018a). The gas dryness ratio (not shown here) also varied  
756 significantly over time for a given well, but in general it did not affect the interpretation,  
757 as values tended to remain within the same “class” (<100 for thermogenic gas, >1000 for  
758 microbial gas).

759 In contrast, isotopic values (CH<sub>4</sub>-δ<sup>13</sup>C and -δ<sup>2</sup>H) were generally very stable over time, with  
760 variations remaining within the uncertainty expected for sampling, handling and analysis  
761 (Rivard et al., 2018a). However, the two wells with the lowest methane concentrations  
762 (Zone 9R and F3) showed significant variations over time (Figure 9). Changes in isotopic  
763 composition due to either mixing of gas sources in varying proportions, or to post-genetic  
764 processes affecting methane, are likely to have a more noticeable effect when methane  
765 concentrations are small. In well F3, the variations were attributed to oxidation (Rivard et  
766 al., 2018a) while in Zone 9R, the main factor is the detection of thermogenic gas with a

767 relatively deep formation gas signature in the first sample of the series (Bordeleau et al.,  
768 2018b). DIC- $\delta^{13}\text{C}$  values were also found to vary significantly over time (not shown here),  
769 especially in wells where methane concentrations were high and where late-stage  
770 methanogenesis was predominant (Rivard et al., 2018a).

771 Therefore, while isotopic values of methane are usually a good and stable indicator of gas  
772 origin in a well, significant variations may occur in some wells and thus monitoring for  
773 both concentration and isotopic values should be carried out for a sufficient period ahead  
774 of any shale gas activities to establish natural variability. Moreover, monitoring of DIC-  
775  $\delta^{13}\text{C}$  may prove very helpful in interpreting the origin of methane, especially when  $\text{CH}_4$ -  
776  $\delta^{13}\text{C}$  values are ambiguous. Most importantly, interpretation of gas origin based on a single  
777 sample from a well could be erroneous if that sample is a punctual anomaly, as was  
778 observed on a few occasions in this study. These results could therefore have important  
779 implications on regulatory or voluntary procedures aiming to define the natural baseline  
780 presence of methane prior to shale gas activities.

781

## 782 **7 Importance of multi-source and multi-discipline data**

783

784 The complex scientific issues associated with the study of potential upward fluid migration  
785 from hydrocarbon reservoirs to shallow aquifers ideally require multisource data and  
786 multidisciplinary expertise. Within the Saint-Édouard project, the approach used integrated  
787 data from and expertise in structural geology, stratigraphy, hydrogeology, geophysics,

788 geomechanics and organic/inorganic geochemistry, which together indicated key elements  
789 to better understand the relations between shallow and deep earth systems. This  
790 multidisciplinary approach involved many research scientists and required intensive  
791 fieldwork and numerous laboratory analyses. Moreover, the access to industry data appears  
792 to be essential for this type of project, since the cost of data from dedicated deep wells  
793 would be prohibitive. The combination of these data allowed an assessment of the integrity  
794 of the intermediate zone (presence or absence of fluid migration pathways) and  
795 characterization of natural gas in shallow groundwater.

796

## 797 **7.1 Integrity of the intermediate zone**

798

799 At first, the geological interpretation from industry deep seismic data provided indications  
800 that fluid pathways linking the shale gas reservoir to shallow aquifers could possibly be  
801 present, especially in the vicinity of the RJC normal fault (Lavoie et al., 2016).  
802 Unfortunately, the shallow seismic survey, which was expected to provide key information  
803 on the presence or absence of faults in the near surface (and if present, their precise  
804 location), did not work well in this region. However, the HTEM survey (see Supplementary  
805 information section) provided further indications of the presence of an anomalous feature  
806 in the first few hundred meters, in the vicinity of this normal fault. Although firm  
807 conclusions could not be drawn,  $^{222}\text{Rn}$  in soil gas and groundwater (see also Supplementary  
808 Information section) indicated possibilities of active upward migration in fault zones,  
809 where slightly higher values were found compared to areas away from faults (Bordeleau et

810 al., 2018c). Therefore, these early surveys justified the need to drill observation wells in  
811 the vicinity of fault zones to provide more focused data close to these geological features.

812 On the other hand, initial geological and hydrogeological data provided indications against  
813 the presence of a fluid migration pathway along the two regional fault zones. The  
814 piezometric map seemed to indicate that groundwater flow was merely occurring from the  
815 Appalachian uplands all the way towards the St. Lawrence River, following topography.  
816 Therefore, the St. Lawrence River had initially been assumed to correspond to the regional  
817 groundwater discharge zone. Also, previous publications on the geological context of this  
818 area had reported lines of evidence of fault sealing based on overpressured conditions and  
819 low water saturation in the Utica Shale, as well as unbalanced fluid pressure on both sides  
820 of the Yamaska fault, which extends northeast into the RJC fault present in our study area  
821 (Chatellier et al., 2013; Séjourné et al., 2013; Konstantinovskaya et al., 2009). Furthermore,  
822 clay gouge was observed in cores drilled in the parautochthonous domain to the south and  
823 is suspected to be present in the RJC normal fault due to the presence of similar shale units  
824 to the north and because clay gouge was also observed in at least two deep wells drilled  
825 into the Yamaska fault zone south-west to the study area (Séjourné et al., 2013), supporting  
826 a lack of significant circulation across the fault.

827 The integration of geophysical (shallow and deep borehole logging), geomechanical,  
828 geological (structure and stratigraphy) and hydrogeological data allowed the  
829 characterization of the fracture network throughout the entire sedimentary succession and  
830 provided a first estimate of hydraulic properties for both the shallow and deep intervals  
831 and, by extension, for the intermediate zone (Ladevèze et al., 2018b). Open natural  
832 fractures in the reservoir (and thus in the intermediate zone) are mainly from one set (FS1).

833 Due to their single orientation, these open fractures are thus poorly interconnected, which  
834 does not favour permeability nor flow towards the surface, even if a higher open fracture  
835 density was observed in the vicinity of thrust faults. Ladevèze et al. (2018b) concluded that  
836 the possibility for the fracture network or fault zones to act as large-scale flow pathways  
837 was very unlikely. Furthermore, the geomechanical stratigraphy (Séjourné, 2017) provided  
838 clear evidence against any significant upward extension of hydraulically-induced fractures  
839 from the brittle Utica Shale into the more ductile Lorraine Group. These findings are in  
840 agreement with the reported overpressured conditions of the Utica Shale (Chatellier et al.,  
841 2013) that indicate a lack of significant natural fluid connectivity with the surface.

842 Groundwater geochemical data provided evidence that upward migration of saline fluids  
843 is occurring in the normal fault zone over a distance in the order of a couple hundreds of  
844 meters (likely 200 to 500 m), but not from as deep as the Utica Shale. Also, the first sample  
845 from well Zone 9R, which had a thermogenic signature, appeared to have a  $\text{CH}_4\text{-}\delta^{13}\text{C}$  value  
846 that is consistent with data from deep shales of the Lorraine Group and not of the Utica  
847 Shale (Bordeleau et al., 2018b). While geological and hydrogeological data alone would  
848 not have detected a fluid migration pathway along the normal fault, geology did provide a  
849 working hypothesis to explain the local increase of permeability compared to the regional-  
850 dominant shale host rock in this area (entrainment of porous and more fractured siltstone  
851 beds into the fault core in the upper part of the intermediate zone), which would allow the  
852 upward migration of deeper brines.

853 Based on the ensemble of data just mentioned, Figure 10 presents the conceptual model for  
854 regional groundwater flow occurring in shallow aquifers and the upper portion of the  
855 intermediate zone. This conceptual model infers that some of the water recharging in the

856 Appalachians would circulate towards the northwest at a certain depth in the intermediate  
857 zone (between 200 and 500 m), where it would gain salinity while flowing within the  
858 intermediate zone. In the thrust fault zone of the parautochthonous domain, it is believed  
859 that a small portion of the flow may be able to pass through at different depths in the more  
860 or less tectonized and fractured thrust slices. This water would then discharge upward in  
861 the more porous and fractured damage zone of the RJC normal fault, where siltstone beds  
862 have likely been dragged. Numerical simulations carried out by Janos et al. (2018) showed  
863 the hydraulic plausibility of this inferred impact of the RJC fault on regional groundwater  
864 flow. Once groundwater reaches the upper, more fractured part of the aquifer, it may cross  
865 the core of the fault and flow downstream (to the northwest), following the general flow  
866 direction towards the St. Lawrence River. The airborne (HTEM) survey, fracture data from  
867 the borehole logging, and geochemical profiles confirmed that the active groundwater flow  
868 zone is in the order of 60 m deep, below which the intermediate zone begins.

869 A summary of the arguments in favor or against the presence of migration pathways,  
870 obtained from each scientific discipline, is presented in Supplementary Table S-2.

871

## 872 **7.2 Methane baseline study**

873

874 One of the main objectives of this study was to provide a baseline characterization of  
875 methane and higher alkanes in shallow groundwater of the Saint-Édouard area, before any  
876 shale gas exploitation occurred. In this respect, the key element of this project was the  
877 combination of geochemical data from: 1) the industry (concerning deep-seated fluids from

878 the Lorraine Group and Utica Shale), 2) shallow groundwater from both residential and  
879 dedicated observation wells, and 3) shallow bedrock cores and cuttings from observation  
880 wells. A wide suite of geochemical, and particularly isotopic parameters provided  
881 indications about the source (microbial versus thermogenic) and origin (shallow depths or  
882 deep units) of dissolved methane in the aquifer, as well as the processes affecting methane.  
883 The processes that affect microbial methane in this region (late-stage methanogenesis,  
884 mixing with thermogenic gas and, to a lesser extent, oxidation) originally resulted in  
885 ambiguous interpretation of thermogenic versus microbial origins, but the use of multiple  
886 lines of evidence helped shed light on the complex history of methane production in the  
887 study area.

888 This multi-isotope approach led to the conclusion that both microbial and thermogenic  
889 methane comes from shallow fractured rock, which is mainly composed of organic-rich  
890 black shales. In Late Ordovician, the latter units were tectonically and stratigraphically  
891 buried under at least 4 km of Paleozoic strata, which provided conditions that allowed the  
892 production of thermogenic methane (Dietrich et al., 2011), before erosion resulted in the  
893 modern landscape. Today, shallow units also have the necessary reducing conditions  
894 (oxygen- and sulfate-free) to support microbial methanogenesis. Analyses of shallow  
895 bedrock cores and cuttings, as well as groundwater monitoring over time, demonstrated  
896 that thermogenic gas and old microbial gas produced in the distant past, remain trapped in  
897 shale pores, and are rapidly released during and shortly after well drilling, as well as very  
898 slowly afterwards (Lavoie et al., 2016; Rivard et al., 2018a). In addition, recent microbial  
899 gas is formed in groundwater, which may locally undergo oxidation.

900

### 901 **7.3 Knowledge gaps and recommendations for future studies**

902

903 The combination of data from multiple disciplines allowed the development of geological  
904 and hydrogeological conceptual models integrating all depths of interest (shallow aquifer,  
905 intermediate zone and deep industry-targeted shale), and thus provided a full evaluation of  
906 the possibility for upward fluid migration from the Utica Shale to the shallow aquifer. As  
907 the intermediate zone was very poorly characterized, the interpretation of the intermediate  
908 zone integrity relied on indirect data. To address the remaining unknowns to carry out a  
909 quantitative assessment of the potential environmental risks of upward migration, drilling  
910 of research observation wells in the intermediate zone would be necessary, as these wells  
911 would provide key information, such as the depth to which upward migration occurs and  
912 actual permeabilities, especially near fault zones. Deep monitoring wells are indeed  
913 considered essential for the development of fundamental geoscience by several authors  
914 (Jackson et al., 2013b; Soeder, 2015; Ryan et al., 2015). Despite these recommendations,  
915 these expensive wells are still too few.

916 Also, the Council of Canadian Academies report (CCA, 2014) on environmental impacts  
917 of shale gas extraction in Canada stressed that appropriate environmental monitoring  
918 approaches have not yet been designed and that monitoring needs to engage independent  
919 experts to gain public trust. The development of a sound methodological approach for the  
920 assessment of shallow aquifer vulnerability to deep industrial activities is the prerequisite  
921 for many jurisdictions to get the social licence to safely develop a shale play. As a first step  
922 in this direction, and while we are conscious that the local geological and hydrogeological  
923 context has a major impact on the results, Table 1 provides recommendations for future

924 projects. Although many of the scientific activities were carried out in an effort to see what  
925 could work best for this project, almost all of them ended up being rated high, as each  
926 provided pieces of information that, once put together, allowed a better understanding of  
927 the system. Table 1 can obviously be adapted according to the available equipment and  
928 expertise available to conduct a project. Finally, to provide a more hands-on example of  
929 the usefulness of each activity, Supplementary Table S-2 presents a summary of new  
930 knowledge generated by this research focussing on its significance for or against the  
931 possibility of large-scale migration in the Saint-Édouard area.

932

Table 1: List of recommended activities, along with their requirement, importance and potential contribution

Activity	Requirement	Importance / potential contribution
Re-processing and interpretation of deep seismic surveys	Have access to industry data.	High / Could provide preliminary information on potential upward migration, especially close to regional fault zones.
HTEM survey and interpretation	<p>Have significant funds.</p> <p>Have a nearly undeformed geological setting: complex geology (e.g. folded rocks) will probably not allow good results.</p> <p>The transect should only cross a minimum number of municipalities and electromagnetic features (e.g., electric lines), otherwise data are unusable in these areas.</p>	<p>Moderate / Could provide a regional shallow survey of the fresh-saline water interface that may not be obtained otherwise.</p> <p>Other data providing indications about lithology or fluid content (e.g. geophysical logs) would allow the verification of the inversion and of its interpretation.</p>
Shallow seismic survey	Have significant funds or have access to in-house equipment and expertise. Make preliminary tests in the study area to see if usable and conclusive to image the first 500 m.	High / Could complement the deep seismic survey to see if faults extend to the surface (or close to).

Geomechanical interpretation	Have access to borehole logging data and core samples from deep oil and gas wells and substantial budget if no expertise among stakeholders.	High / Could provide geomechanical properties that allows a better understanding of the behavior of induced fractures into the IZ in case of hydraulic fracturing and of specific units (e.g. shales of the Utica Shale and of the Lorraine Group in this case).
Drilling of observation wells	Have a substantial budget.	Very high / Main interest of having observation wells is to be able to perform all kinds of measurements (e.g. borehole logging, hydraulic tests, sampling at specific depths, geochemical profiling). Observation wells can be complemented by residential wells for a better spatial coverage and to see if they react similarly over time.
Characterization of the fracture network	Have access to borehole logging data from shallow and deep wells (and, if possible, intermediate depths)	High / Obtain information on fracture interconnection and permeability over the entire succession to assess risk of upward migration. Since few data are usually available in the IZ and this zone controls shallow aquifer vulnerability to deep activities, it is important to characterize intervals for which data are available and try to see if the results are applicable to the IZ.
Characterization of hydraulic properties	Complete a fracture network characterization from the gas reservoir to the surface based on shallow and deep	High / As the objective of the project is to study the potential for upward fluid migration, hydraulic

	<p>well logging data and visited outcrops. Perform hydraulic tests in shallow wells.</p> <p>Have access to fracture aperture data from the industry or be able to estimate them from available data.</p> <p>Ideally, have access to pressure values at different depths to estimate the vertical hydraulic gradient and to hydraulic properties (e.g. drill-stem tests) from the industry.</p>	<p>properties within the different intervals, including the IZ, is also very important. Estimates from data apertures and frequency of open fractures provide best guests for porosity and permeability at depth if the latter are not already available. <i>In situ</i> hydraulic tests at depth would provide key data, necessary to carry out a quantitative assessment of shallow aquifer vulnerability to deep industrial activities.</p>
<p>Groundwater geochemistry</p>	<p>A moderate budget is needed for the baseline study, both for human resources and laboratory analyses. The latter would include, at the very least, major ions and metals, and alkane concentrations and <math>-\delta^{13}\text{C}</math>. To allow a thorough interpretation, alkane-<math>\delta^2\text{H}</math> and DIC-<math>\delta^{13}\text{C}</math> are also highly recommended. If possible, DIC-<math>^{14}\text{C}</math>, <math>^3\text{H}</math>, and <math>\text{H}_2\text{O}-\delta^2\text{H}</math> and <math>-\delta^{18}\text{O}</math> are also recommended.</p> <p>Other, less traditional indicators have proven to be useful in this study, such as <math>\text{CH}_4-^{14}\text{C}</math> and <math>^{36}\text{Cl}</math>. A good spatial coverage, including a finer distribution in the vicinity of regional fault zones, are ideal. A combination of observation wells that can be</p>	<p>Very High / GW geochemistry allows the indirect verification of possible upward fluid migration, given that sampled wells are adequately located.</p>

	thoroughly investigated and residential wells that increase the density of spatial coverage is recommended.	
Rock geochemistry	Have access to drill cuttings or core samples (some placed in Isojars® for hydrocarbon composition analyses), and well preserved deep core samples or gas analyses from the industry for comparison.	Useful only if hydrocarbons are detected in GW. In this case, it rates High / Essential if one wants to make a comparison between GW and rock organic geochemistry to provide evidence that gas comes from the shallow aquifer itself, or from deep formations.
Soil geochemistry (see Supplementary Information section)	Useful only if hydrocarbons are present in GW. A thin, permeable surficial sediment cover may provide clearer indications of potential fluid migration.	Moderate / Could provide preliminary information on potential upward migration, especially close to regional fault zone.
Groundwater monitoring	Moderate budget and time is required for regular sampling campaigns. GW monitoring should be carried before, during and after shale gas (or any deep industrial) activities; it should include alkane concentrations and isotopic composition, as both can vary over time and these fluctuations could be misleading once oil and gas activities start. Monitoring of DIC- $\delta^{13}\text{C}$ can also provide important information	Very high / Monitoring data will provide reliable data in case a complaint is logged against the industry. As more data will be collected, this will help develop appropriate regulations for given areas.  Such monitoring provides indications of the natural variability of methane concentrations and isotopic composition, which may help provide firmer indications

	on microbial processes affecting methane. Monitoring prior to any oil and gas activities should be carried out for at least a year, two years if possible.	of impacts on groundwater from industrial subsurface activities.
Use of downhole gas sensors (see SI section for work carried out)	Have a substantial budget or develop in-house sensors (or collaboration with people doing research in this field).	While these sensors would be necessary to collect shorter-term data on methane concentrations, it is probably better to wait until technology and methodology is ready.
Pore-water analyses from shallow and deep shale samples	Have access to this type of analyses (exclusively carried out in a few universities worldwide). Core samples must not be too tight (potential for these analyses is severely limited in tight shales).	Low / Could provide information on brines and hydrocarbons in pores at different depths.

## 935 **8 Conclusion**

936

937 Knowledge of potential impacts of deep unconventional reservoir development on shallow  
938 aquifers is a major issue for the hydrocarbon industry, mainly due to environmental  
939 concerns related to groundwater contamination, especially in regions where large-scale  
940 unconventional hydrocarbon activities have never taken place. This paper presented an  
941 overview of the work carried out during a 4-year multidisciplinary project on the  
942 assessment of shallow aquifer vulnerability to deep shale gas activities through upward  
943 fluid migration, in a region where only little exploration has occurred so far. The Saint-  
944 Édouard area, overlying the Utica Shale in eastern Canada (more specifically in the St.  
945 Lawrence Lowlands, province of Quebec), had been selected notably because the shale gas  
946 exploration well drilled in this locality was the most promising well in the St. Lawrence  
947 Lowlands, and importantly, it was possible to have access to data from the operator.

948 Potential links between deep geological units targeted by the industry and surficial aquifers  
949 are usually not well documented or understood. Aquifer protection thus strongly depends  
950 on a better geological and hydrogeological knowledge of these zones. As data have  
951 generally not been acquired in the past within the intermediate zone, scientific information  
952 must be gained through indirect data, ideally from multiple sources. In this project,  
953 extensive fieldwork was carried out and a wide range of data were collected and analysed  
954 including geological, geophysical, geomechanical, geochemical and hydrogeological data.  
955 These data were both interpreted individually and in combination with data from the other  
956 disciplines.

957 Results showed that groundwater in this area generally contains methane, sometimes in  
958 very high concentrations, and occasionally some ethane and propane. Of the 44 residential  
959 and observation wells that were sampled, 36% had methane concentrations above 7 mg/L,  
960 the alert threshold for the Department of Environment of Quebec. These concentrations, as  
961 well as the sources of methane and processes affecting it, were shown to be variable in  
962 space and/or time. Most methane in this region is of microbial origin, but thermogenic gas  
963 was found in 15% of the wells. Rock organic geochemistry showed that the shallow  
964 bedrock itself is the source of both types of gas found in groundwater. While evidence of  
965 local upward fluid migration of brines from the intermediate zone was found in the vicinity  
966 of a normal fault, aquifers of this area appear to be well protected against contamination  
967 from industrial activities carried out at depth, based on the acquired data and interpretation.  
968 Nonetheless, the interpretation inferred from the available data, combined to the lack of  
969 direct data in the intermediate zone, indicate that care should be taken should drilling of  
970 gas wells be resumed, and until new data specific to the fault zones are available, hydraulic  
971 fracturing should be avoided in their vicinity.

972 The specific results and conclusions presented here are valid only for the study area and  
973 should not be directly extended to other regions, even within the St. Lawrence Lowlands.  
974 Nonetheless, the methodology developed within this project and recommendations made  
975 for future similar projects should likely be useful to other regions where deep industrial  
976 activities are planned, and it is hoped that it will serve as a basis to help research scientists  
977 develop a more in-depth methodology. Overall, collaborative and integrated projects  
978 between the government, academia and industry are necessary to quantitatively assess  
979 impacts or risks for shallow fresh groundwater for such environmental studies.

980

981 **Acknowledgements**

982

983 The authors are very grateful to well owners of the study area, as well as to Talisman  
984 Energy/Repsol Canada, and especially to Marianne Molgat, for giving us access to their  
985 data. Without them, this project could not have been carried out. Authors would also like  
986 to thank Natural Resources Canada, namely the PERD and Eco-EII programs from the  
987 Energy Sector and the Environmental Geoscience program of the Minerals and Lands  
988 Sector for their financial support. Support from three Quebec ministries (Ministère du  
989 Développement durable, de l'Environnement et de la Lutte contre les Changements  
990 climatiques, Ministère des Forêts, de la Faune et des Parcs, Ministère de l'Énergie et des  
991 Ressources naturelles), from the municipality of Saint-Édouard and from the Regional  
992 municipality (MRC) of Lotbinière was greatly appreciated and useful. The authors finally  
993 wish to acknowledge the work of Dr. Steve Grasby and two anonymous reviewers for their  
994 constructive and valuable comments. This is GSC contribution # 20180257.

995

996 **References**

997

998 BAPE. 2010. Comparaison des shales d'Utica et de Lorraine avec des shales en  
999 exploitation, Réponse de l'APGQ aux questions de la Commission du BAPE sur les gaz de  
1000 schiste. Available at:  
1001 [http://www.bape.gouv.qc.ca/sections/mandats/Gaz\\_de\\_schiste/documents/DB25%20table](http://www.bape.gouv.qc.ca/sections/mandats/Gaz_de_schiste/documents/DB25%20table)  
1002 [au%20de%20shales.pdf](http://www.bape.gouv.qc.ca/sections/mandats/Gaz_de_schiste/documents/DB25%20table) (accessed February 2017). Bureau d'Audiences Publiques sur  
1003 l'Environnement (BAPE) DB25  
1004 BAPE. 2014. Les enjeux liés à l'exploration et l'exploitation du gaz de schiste dans le shale  
1005 d'Utica des basses-terres du Saint-Laurent. Rapport d'enquête et d'audience publique.  
1006 Bureau d'audiences publiques sur l'environnement (BAPE) Bibliothèque et Archives  
1007 nationales du Québec, Québec City, Canada Report 307: 546.  
1008 Bear, J. 1993. 1 - Modeling Flow and Contaminant Transport in Fractured Rocks. Flow  
1009 and Contaminant Transport in Fractured Rock, Academic Press,  
1010 Oxford <http://dx.doi.org/10.1016/B978-0-12-083980-3.50005-X>. p 1-37.  
1011 Bense, V.F., Gleeson, T., Loveless, S.E., Bour, O., Scibek, J. 2013. Fault zone  
1012 hydrogeology. Earth-Science Reviews, 2013, 171-192.  
1013 Bernard, B.B., Brook, J.M., Sackett, W.M. 1976. Natural gas seepage in the Gulf of  
1014 Mexico, Earth Planet. Sci. Lett. 31, 48–54.  
1015 Birdsell, D.T., Rajaram, H., Dempsey, D., Viswanathan, H.S. 2015. Hydraulic fracturing  
1016 fluid migration in the subsurface: a review and expanded modeling results. Water  
1017 Resources Research, 51:7159–7188. <https://doi.org/10.1002/2015WR017810>

1018 Bordeleau, G., Rivard, C., Lavoie, D., Lefebvre, R., Malet, X., Ladevèze, P. 2018a.  
1019 Geochemistry of groundwater in the Saint-Édouard area, Quebec, Canada, and its influence  
1020 on the distribution of methane in shallow aquifers. *Applied Geochemistry*, 89: 92-108.

1021 Bordeleau, G., Rivard, C., Lavoie, D., Lefebvre, R., Ahad, J., Mort, A., Xu, X., 2018b, A  
1022 multi-isotope approach to determine the origin of methane and higher alkanes in  
1023 groundwater of the Saint-Édouard area, eastern Canada, *Environmental Geoscience*, in  
1024 press.

1025 Bordeleau, G., Rivard, C., Lavoie, D., Lefebvre, D., Malet, X. 2018c. Geochemical study  
1026 of the Saint-Édouard area, southern Quebec, Geological Survey of Canada, Open File 8505  
1027 (submitted).

1028 Botner, E.C., Townsend-Small, A., Nash, D.B., Xu, X., Schimmelmann, A., Miller, J.H.  
1029 2018. Monitoring concentration and isotopic composition of methane in groundwater in  
1030 the Utica Shale hydraulic fracturing region of Ohio, *Environmental Monitoring and*  
1031 *Assessment* 190:322, <https://doi.org/10.1007/s10661-018-6696-1>.

1032 Bouwer, H., Rice, R.C. 1976. A slug test for determining hydraulic conductivity of  
1033 unconfined aquifers with completely or partially penetrating wells. *Water Resources*  
1034 *Research* 12(3):423-428.

1035 Caine, J.S., Evans, J.P., Forster, C.B. 1996. Fault zone architecture and permeability  
1036 structure. *Geology*, 24, 1025-1028.

1037 Castonguay, S., Dietrich, J., Lavoie, D., Laliberté, J.-Y. 2010. Structure and petroleum  
1038 plays of the St. Lawrence Platform and Appalachians in southern Quebec: insights from

1039 interpretation of MRNQ seismic reflection data. *Bulletin Canadian Petroleum Geology*, 58,  
1040 219–234.

1041 CCA. 2014 Environmental impacts of shale gas extraction in Canada. Available at  
1042 [http://www.scienceadvice.ca/uploads/eng/assessments%20and%20publications%20and%20news%20releases/shale%20gas/shalegas\\_fullreporten.pdf](http://www.scienceadvice.ca/uploads/eng/assessments%20and%20publications%20and%20news%20releases/shale%20gas/shalegas_fullreporten.pdf) (accessed February 2017).  
1043 Council of Canadian Academies (CCA): 292

1044

1045 Chatellier, J.-Y., Flek, P., Molgat, M., Anderson, I., Ferworn, K., Lazreg Larsen, N., Ko,  
1046 S. 2013. Chapter 3: Overpressure in Shale Gas: When Geochemistry and Reservoir  
1047 Engineering Data Meet and Agree. *AAPG Special Volumes Memoir*, 103: Critical  
1048 Assessment of Shale Resource Plays: 45-69

1049

1049 Chen, Z., Lavoie, D. and Malo, M. 2014. Geological characteristics and petroleum resource  
1050 assessment of Utica Shale, Quebec, Canada. *Geological Survey of Canada, Open File 7606*,  
1051 43 p.

1052

1052 Chen, Z., Lavoie, D., Malo, M., Jiang, C., Sanei, H., Ardakani, O.H. 2017. A dual-porosity  
1053 model for evaluating petroleum resource potential in unconventional tight-shale plays with  
1054 application to Utica Shale, Quebec (Canada). *Marine and Petroleum Geology*, 80: 333-348.

1055

1055 Clark, T.H., Globensky, Y. 1973. Portneuf et parties de St-Raymond et de Lyster - Comtés  
1056 de Portneuf et de Lotbinière, Ministère des Richesses Naturelles - Direction Générale des  
1057 Mines, Rapport Géologique RG-148, 110 p.

1058

1058 Coleman, N.P., McElreath, D. 2012. Short-term Intra-Well Variability in Methane  
1059 Concentrations from Domestic Well Waters in Northeastern Pennsylvania, *AAPG Search*

1060 and Discovery Article #90154©2012, AAPG Eastern Section Meeting: Stray Gas  
1061 Incidence & Response Forum, Cleveland, Ohio, 24-26 July 2012,  
1062 [http://www.gwpc.org/sites/default/files/event-sessions/Coleman\\_Nancy.pdf](http://www.gwpc.org/sites/default/files/event-sessions/Coleman_Nancy.pdf).

1063 Crow, H.L., Ladevèze, P. 2015. Downhole geophysical data collected in 11 boreholes near  
1064 St.-Édouard-de-912 Lotbinière, Québec. Geological Survey of Canada, Open File 7768:  
1065 48p. DOI 10.4095/297047.

1066 Currell, M., Banfield, D., Cartwright, I, Cendón, D.I. 2017. Geochemical indicators of the  
1067 origins and evolution of methane in groundwater: Gippsland Basin, Australia. Environ Sci  
1068 Pollut Res (2017) 24: 13168-13183.

1069 Darrah, T. H.; Vengosh, A.; Jackson, R. B.; Warner, N. R.; Poreda, R. J. 2014. Noble gases  
1070 identify the mechanisms of fugitive gas contamination in drinking-water wells overlying  
1071 the Marcellus and Barnett Shales. Proc. Natl. Acad. Sci. U. S. A. 111, 14076–14081.

1072 Dietrich, J., Lavoie, D., Hannigan, P., Pinet, N., Castonguay, S., Giles, P., Hamblin, A.P.  
1073 2011. Geological Setting and Resource Potential of Conventional Petroleum Plays in  
1074 Paleozoic Basins in Eastern Canada. Bulletin of Canadian Petroleum Geology, 59; 54-84.

1075 Dusseault, M., Jackson R. 2014 Seepage pathway assessment for natural gas to shallow  
1076 groundwater during well stimulation, in production, and after abandonment.  
1077 Environmental Geosciences, 21(3):107-126.

1078 EPA. 2016. Hydraulic Fracturing for Oil and Gas: Impacts from the Hydraulic Fracturing  
1079 Water Cycle on Drinking Water Resources in the United States (Final Report). US  
1080 Environmental Protection Agency (EPA), Washington, DC EPA/600/R-16/236F: 666

1081 Esterhuysen, S. 2017. Developing a groundwater vulnerability map for unconventional oil  
1082 and gas extraction: a case study from South Africa, *Environmental Earth Sciences*. 76:626,  
1083 DOI 10.1007/s12665-017-6961-6.

1084 Faulkner, D.R., Jackson, C.A.L., Lunn, R.J., Schlische, R.W., Shipton, Z.K., Wibberley,  
1085 C.A.J., Withjack M.O. 2010. A review of recent developments concerning the structure,  
1086 mechanics and fluid flow properties of fault zones. *Journal of Structural Geology*, 1557-  
1087 1575.

1088 Gale, J.F., Reed, R.M., Holder, J. 2007. Natural fractures in the Barnett Shale and their  
1089 importance for hydraulic fracture treatments. *AAPG Bulletin* 91: 603-622.

1090 Gale, J., Ukar, E., Elliott, S.J., Wang, Q. 2015. Bedding-Parallel Fractures in Shales:  
1091 Characterization, Prediction and Importance. *AAPG Annual Convention and Exhibition*,  
1092 Denver, CO., USA, May 31 - June 3, 2015.

1093 Gassiat, C., Gleeson, T., Lefebvre, R., McKenzie, J. 2013. Hydraulic fracturing in faulted  
1094 sedimentary basins: numerical simulation of potential contamination of shallow aquifers  
1095 over long time scales. *Water Resources Research* 49:8310–8327.  
1096 <https://doi.org/10.1002/2013wr014287>.

1097 Globensky, Y. 1987. *Géologie des Basses-Terres du Saint-Laurent, Québec*: Ministère des  
1098 Richesses naturelles, Québec, MM 85-02, 63 pp.

1099 Gorody, A.W. 2012. Factors affecting the variability of stray gas concentration and  
1100 composition in groundwater, *Environmental Geosciences*, 19(1): 17–31.

1101 Grasby, S.E., Ferguson, G., Brady, A., Sharp, C., Dunfield, P., McMechan, M. 2016. Deep  
1102 groundwater circulation and associated methane leakage in the northern Canadian Rocky  
1103 Mountains. *Applied Geochemistry* 68: 10-18 DOI  
1104 <https://doi.org/10.1016/j.apgeochem.2016.03.004>

1105 Harkness, J.S., Darrah, T.H., Warner, N.R., Whyte, C.J., Moore, M.T., Millot, R.,  
1106 Kloppman, W., Jackson, R.B., Vengosh, A., 2017. The geochemistry of naturally occurring  
1107 methane and saline groundwater in an area of unconventional shale gas development.  
1108 *Geochimica et Cosmochimica Acta*, 208 : 302-334, doi:  
1109 <http://dx.doi.org/10.1016/j.gca.2017.03.039>.

1110 Hounslow, A. W., 1995. *Water Quality Data Analysis and Interpretation*. Lewis Publishers,  
1111 Boca Raton, FL, 379 p.

1112 Humez, P., Mayer, B., Nightingale, M., Ing, J., Becke,r V, Jones, D. 2015. An 8-year record  
1113 of gas geochemistry and isotopic composition of methane during baseline sampling at a  
1114 groundwater observation well in Alberta (Canada). *Hydrogeology Journal*, doi:  
1115 [10.1007/s10040-015-1319-1](https://doi.org/10.1007/s10040-015-1319-1).

1116 Humez, P., B. Mayer, J. Ing, M. Nightingale, V. Becker, A. Kingston, O. Akbilgic, Taylor,  
1117 S. 2016, Occurrence and origin of methane in groundwater in Alberta (Canada): Gas  
1118 geochemical and isotopic approaches: *Science of the Total Environment*, v. 541, p. 1253-  
1119 1268, doi: [10.1016/j.scitotenv.2015.09.055](https://doi.org/10.1016/j.scitotenv.2015.09.055).

1120 Hyder, Z. Butler, J.J. McElwee, C., Liu, W. 1994. Slug tests in partially penetrating wells.  
1121 *Water Resources Research* 30(11): 2945-2957.

1122 Janos, D., Molson, J., Lefebvre, R. 2018. Regional groundwater flow dynamics and  
1123 residence times in Chaudière-Appalaches, Québec, Canada: Insights from numerical  
1124 simulations. Online 15 April 2018, Canadian Water Resources Journal, 26 pp, doi:  
1125 10.1080/07011784.2018.1437370.

1126 Jackson, R.B., Vengosh, A., Darrah, T.H., Warner, N.R., Down, A., Poredac, R.J., Osborn,  
1127 S.G., Zhao, K., Karra, J.D. 2013a. Increased stray gas abundance in a subset of drinking  
1128 water wells near Marcellus shale gas extraction. Proc. Natl. Acad. Sci., U. S. A. 110:  
1129 11250–11255.

1130 Jackson, R. E.; Gorody, A. W.; Mayer, B.; Roy, J. W.; Ryan, M. C.; Van Stempvoort, D.  
1131 R. 2013b. Groundwater protection and unconventional gas extraction: the critical need for  
1132 field based hydrogeological research. *Ground Water* 3, 51, 488–510.

1133

1134 Kissinger, A., Helmig, R., Ebigbo, A., Class, H., Lange, T., Sauter, M., Heitfeld, M.,  
1135 Klünker, J., Jahnke, W. 2013. Hydraulic fracturing in unconventional gas reservoirs: risks  
1136 in the geological system, part 2. *Environmental Earth Sciences* 70: 3855-3873 DOI  
1137 10.1007/s12665-013-2578-6.

1138 Konstantinovskaya, E.A., Rodriguez, D., Kirkwood, D., Harris, L.B., Thériault, R., 2009.  
1139 Effects of basement structure, sedimentation and erosion on thrust wedge geometry: an  
1140 example from the Quebec Appalachians and Analogue models. *Bulletin of Canadian*  
1141 *Petroleum Geology*, 57 : 34-62.

1142 Ladevèze, P. 2017. Aquifères superficiels et gaz de shale : le rôle des failles et réseaux de  
1143 fractures naturelles sur la circulation des fluides. (Surficial aquifers and shale gas : role of  
1144 faults and natural fracture networks on fluid circulation), Ph. D. thesis, Institut national  
1145 de la recherche scientifique - Centre Eau Terre Environnement (INRS-ETE), 223 p.

1146 Ladevèze, P., Rivard, C., Lefebvre, R., Lavoie, D., Parent, M., Malet, X., Bordeleau, G.,  
1147 Gosselin, J.S. 2016. Travaux de caractérisation hydrogéologique dans la plateforme  
1148 sédimentaire du Saint-Laurent, région de Saint-Édouard-de-Lotbinière, Québec, Dossier  
1149 public 8036, 2016; 112 pages, doi:10.4095/297891.

1150 Ladevèze, P., Séjourné, S., Rivard, C., Lefebvre, R., Lavoie, D., Rouleau, A. 2018a.  
1151 Defining the natural fracture network in a shale gas play and its cover succession; the case  
1152 of the Ordovician Utica Shale in eastern Canada, *Structural Geology*, 108; 157-170.

1153 Ladevèze, P., Rivard, C., Lavoie, D., Séjourné, S., Lefebvre, R., Bordeleau, G. 2018b. Fault  
1154 and natural fracture control on upward fluid migration: insights from a shale gas play in  
1155 the St. Lawrence Platform, Canada, *Hydrogeology Journal*, on line:  
1156 [https://www.springerprofessional.de/en/fault-and-natural-fracture-control-on-upward-](https://www.springerprofessional.de/en/fault-and-natural-fracture-control-on-upward-fluid-migration-ins/16134850)  
1157 [fluid-migration-ins/16134850](https://www.springerprofessional.de/en/fault-and-natural-fracture-control-on-upward-fluid-migration-ins/16134850).

1158 Lavoie, D. 2008. Appalachian Foreland Basin of Canada, in *Sedimentary Basins of the*  
1159 *World*, Edited by A. Miall, Elsevier, 65-103.

1160 Lavoie, D., Desrochers, A., Dix, G., Knight, I., Salad Hersi, O. 2012. The great American  
1161 carbonate bank in eastern Canada: an overview, in: Derby, J.R., Fritz, R.D., Longacre,  
1162 S.A., Morgan, W.A., Sternbach, C.A. (Eds.), *The Great American Carbonate Bank: The*

1163 Geology and Economic Resources of the Cambrian–Ordovician Sauk Megasequence of  
1164 Laurentia: AAPG Memoir 98; 499–523.

1165 Lavoie, D., Rivard, C., Lefebvre, R., Séjourné, S., Thériault, R., Duchesne, M. J., Ahad, J.  
1166 M. E., Wang, B., Benoit, N., Lamontagne, C. 2014. The Utica Shale and gas play in  
1167 southern Quebec: Geological and hydrogeological syntheses and methodological  
1168 approaches to groundwater risk evaluation. *International Journal of Coal Geology*, 126;  
1169 77–91.

1170 Lavoie, D., Pinet, N., Bordeleau, G., Ardakani, O.H., Ladevèze, P., Duchesne, M.J.,  
1171 Rivard, C., Mort, A., Brake, V.I., Sanei, H., Malet, X. 2016. The Upper Ordovician black  
1172 shales of southern Quebec (Canada) and their significance for naturally occurring  
1173 hydrocarbons in shallow groundwater. *International Journal of Coal Geology*, 158: 44-64.

1174 LeDoux, S.T.M. Szykiewicz, A, Faiia, A.M., Mayes. M.A., McKinney, M.L., Dean, W.G.  
1175 2016. Chemical and isotope compositions of shallow groundwater in areas impacted by  
1176 hydraulic fracturing and surface mining in the Central Appalachian Basin, Eastern United  
1177 States, *Applied Geochemistry*, 71: 73-85.

1178 Lefebvre, R. 2017. Mechanisms leading to potential impacts of shale gas development on  
1179 groundwater quality. *WIREs Water*, 4(1), 15 pages. doi: 10.1002/wat2.1188.

1180 Légaré-Couture G., Parent M., Lefebvre R. 2018. Cartographie des formations  
1181 superficielles de la région de Chaudière-Appalaches, 1 :100 000 scale, in preparation.

1182 McIntosh, J. C., Grasby, S. E., Hamilton, S. M., Osborn, S. G. 2014. Origin, distribution  
1183 and hydrogeochemical controls on methane occurrences in shallow aquifers, southwestern

1184 Ontario, Canada. *Appl. Geochem.*, 50: 37–52, doi:  
1185 <http://dx.doi.org/10.1016/j.apgeochem.2014.08.001>.

1186 McMahon, P.B., Belitz, K., Barlow, J.R.B., Jurgens, B.C. 2017. Methane in aquifers used  
1187 for public supply in the United States, *Applied Geochemistry*, 84: 337-347

1188 McMahon, P.B., Caldwell, R.R., Galloway, J.M., Valder, J.F., Hunt, A.G. 2014. Quality  
1189 and age of shallow groundwater in the Bakken Formation production area, Williston Basin,  
1190 Montana and North Dakota, *Ground Water*, 53 Suppl 1:81-94. doi: 10.1111/gwat.12296.

1191 Molofsky, L.J., Connor, J.A., Wylie, A.S., Wagner, T., Farhat, S.K. 2013. Evaluation of  
1192 methane sources in groundwater in northeastern Pennsylvania: *Groundwater*, v. 51, no 3,  
1193 p. 333–349.

1194 Molofsky, L.J., Richardson, S.D., Gorody, A.W., Baldassare, F., Black, J.A., McHugh,  
1195 T.E., Connor, J.A. 2016. Effect of Different Sampling Methodologies on Measured  
1196 Methane Concentrations in Groundwater Samples. *Ground Water*, 24: 1-12, doi:  
1197 10.1111/gwat.12415.

1198 Moritz, A., Helie, J.-F., Pinti, D., Larocque, M., Barnatche, D., Retailleau, S., Lefebvre,  
1199 R., Gelinas. Y. 2015. Methane baseline concentrations and sources in shallow aquifers  
1200 from the shale gas-prone region of the St. Lawrence Lowlands (Quebec, Canada). 2015.  
1201 *Environ. Sci. Technol.*, 49(7):4765-71. doi: 10.1021/acs.est.5b00443.

1202 Nicot, J.P., Larson T., Darvari R., Mickler P., Sloten M., Aldridge J., Uhlman K., Costley  
1203 R. 2017a. Controls on methane occurrences in shallow aquifers overlying the Haynesville

1204 Shale gas field, East Texas. *Groundwater*, 55 (4): 443–454.  
1205 <https://doi.org/10.1111/gwat.12500>

1206 Nicot, J.P., Larson, T., Darvari, R., Mickler, P., Uhlman, K., Costley, R. 2017b. Controls on  
1207 Methane Occurrences in Aquifers Overlying the Eagle Ford Shale Play, South Texas,  
1208 *Groundwater*, 55 (4): 455–468.

1209 Nicot, J.P., Mickler, P., Larson, T., Castro, M.C., Darvari, R., Uhlman, K., Costley, R.  
1210 2017c. Methane Occurrences in Aquifers Overlying the Barnett Shale Play with a Focus  
1211 on Parker County, Texas, *Groundwater*, 55 (4): 469–481.

1212 Nowamooz, A., Lemieux, J.M., Molson, J., Therrien, R. 2014. Numerical investigation of  
1213 methane and formation fluid leakage along the casing of a decommissioned shale gas well.  
1214 *Water Resour Res* 2015, 51:4592–4622.

1215 Occhietti, S., Richard, P.J. 2003. Effet réservoir sur les âges  $^{14}\text{C}$  de la Mer de Champlain à  
1216 la transition Pléistocène-Holocène : révision de la chronologie de la déglaciation au Québec  
1217 méridional. *Géographie physique et Quaternaire*, 57 (2-3), 115-138.

1218 Osborn, S.G., Vengosh, A., Warner, N. R., Jackson, R. B. 2011. Methane contamination  
1219 of drinking water accompanying gas-well drilling and hydraulic fracturing, *Proc. Natl.*  
1220 *Acad. Sci. U. S. A.*, 108, 8172–8176.

1221 Pinet, N., Duchesne, M., Lavoie, D., Bolduc, A., Long, B. 2008. Surface and subsurface  
1222 signatures of gas seepage in the St. Lawrence Estuary (Canada): Significance to  
1223 hydrocarbon exploration. *Marine and Petroleum Geology* 25, 271-288.

1224 Puls, R.W., Barcelona, M.J. 1996. Low-flow (minimal drawdown) groundwater sampling  
1225 procedures. EPA Ground Water Issue, EPA/540/S-95/50, pp 12.

1226 Pugin, A. J.-M., Pullan, S. E. and Hunter, J. A., 2009. Multicomponent high-resolution  
1227 seismic reflection profiling, *The Leading Edge*, 28, 1248–1261.

1228 Reagan, M.T., Moridis, G.J., Keen, N.D., Johnson, J.N. 2015. Numerical simulation of the  
1229 environmental impact of hydraulic fracturing of tight/shale gas reservoirs on near-surface  
1230 groundwater: Background, base cases, shallow reservoirs, short-term gas, and water  
1231 transport. *Water Resources Research* 51: 2543-2573 DOI 10.1002/2014wr016086.

1232 Raynauld, M., Peel, M., Lefebvre, R., Molson, J., Crow, H., Ahad, J., Ouellet, M.,  
1233 Aquilina, L., 2016. Understanding shallow and deep flow for assessing the risk of  
1234 hydrocarbon development to groundwater quality. Online 25 September 2016, Special  
1235 issue on ‘Basin hydrodynamics & Resources’, *J. of Marine and Petroleum Geology*, 78C,  
1236 728-737, doi: 10.1016/j.marpetgeo.2016.09.026

1237 Rivard, C., Bordeleau, G., Lavoie, D., Lefebvre, R., Malet, X. 2018a. Methane variations  
1238 in groundwater over time, *Hydrogeology Journal*, 26: 533–551,  
1239 <https://doi.org/10.1007/s10040-017-1677-y>.

1240 Rivard, C., Bordeleau, G., Lavoie, D., Lefebvre, R., Malet, X. 2018b. Can groundwater  
1241 sampling techniques influence methane concentrations and isotopes?, *Environmental*  
1242 *Monitoring and Assessment Journal*, 190: 191, [https://doi.org/10.1007/s10661-018-6532-](https://doi.org/10.1007/s10661-018-6532-7)  
1243 [7](https://doi.org/10.1007/s10661-018-6532-7).

1244 Ryan, C., Alessi, D., Mahani, A.B., Cahill, A., Cherry, J., Eaton, D., Evans, R., Farah, N.,  
1245 Fernandes, A., Forde, O., Humez, P., Kletke, S., Ladd, B., Lemieux, J.M., Mayer, B.,  
1246 Mayer, K.U., Molson, J., Muehlenbachs, L., Nowamooz, A., Parker, B. (2015) Subsurface  
1247 Impacts of Hydraulic Fracturing: Contamination, Seismic Sensitivity, and Groundwater  
1248 Use and Demand Management, Canadian Water Network, CWN HF-KI Subsurface  
1249 Impacts Report, 149 pp.

1250 Séjourné, S., Lefebvre, R., Malet, X., Lavoie, D. 2013. Synthèse géologique et  
1251 hydrogéologique du Shale d'Utica et des unités sus-jacentes (Lorraine, Queenston et  
1252 dépôts meubles), Basses- Terres du Saint-Laurent, Québec. Commission Géologique du  
1253 Canada, Dossier Public 7338:165.

1254 Séjourné, S. 2016. Étude des données géomécaniques de laboratoire des carottes d'un  
1255 puits pétrolier et gazier (Talisman, Saint-Édouard No 1), région de Saint-Édouard,  
1256 Québec; Commission géologique du Canada, Dossier public 7893, 2016; 54 pages,  
1257 doi:10.4095/297780.

1258 Séjourné, S., 2017. Étude géomécanique du Shale d'Utica et de sa couverture sédimentaire  
1259 d'après les puits pétroliers et gaziers de la région de Saint-Édouard-de-Lotbinière, Québec;  
1260 Commission géologique du Canada, Dossier public 8196, 54 p. doi: 10.4095/299662.

1261 Sherwood, O.A., Rogers, J.D., Lackey, G., Burke, T.L., Osborn, S.G., Ryan, J.N. 2016.  
1262 Groundwater methane in relation to oil and gas development and shallow coal seams in the  
1263 Denver-Julesburg Basin of Colorado, PNAS, 113(30): 8391–8396,  
1264 <http://www.pnas.org/content/113/30/8391.full>, doi: 10.1073/pnas.1523267113.

1265 Siegel, D.I., Azzolina, N.A., Smith, B.J., Perry, E.A., Bothun, R.L. 2015. Methane  
1266 Concentrations in Water Wells Unrelated to Proximity to Existing Oil and Gas Wells in  
1267 Northeastern Pennsylvania, *Environ. Sci. Technol.*, 49 (7), pp 4106–4112, doi:  
1268 10.1021/es505775c.

1269 Smith, B., Becker, M., Siegel, D. 2016. Temporal variability of methane in domestic  
1270 groundwater wells, northeastern Pennsylvania, *Environmental Geosciences*, 23(1): 49–  
1271 80.Snow DT (1968) Rock fracture spacings, openings, and porosities. *Journal of Soil*  
1272 *Mechanics & Foundations Div.*

1273 Snow, D.T. 1968. Rock fracture spacings, openings, and porosities. *Journal of the Soil*  
1274 *Mechanics and Foundations Division*, 94(1): 73-92.

1275 Soeder, D. J. 2015. Adventures in groundwater monitoring: Why has it been so difficult to  
1276 obtain groundwater data near shale gas wells? *Environmental Geosciences*, 22 (4), 139-  
1277 148.

1278 Soeder, D.J., Sharma, S., Pekney N., Hopkinson, L., Dilmore, R., Kutchko, B., Stewart, B.,  
1279 Carter, K., Hakala, A., Capo, R. 2014. An approach for assessing engineering risk from  
1280 shale gas wells in the United States. *International Journal of Coal Geology*, 126:4–19.

1281 Tazaz, A. M., B. M. Bebout, C. A. Kelley, J. Poole, Chanton, J. P.. 2013. Redefining the  
1282 isotopic boundaries of biogenic methane: Methane from endoevaporites: *Icarus*, v. 224 no.  
1283 2, p. 268-275.

1284 Thériault, R. 2012. Caractérisation du Shale d'Utica et du Groupe de Lorraine, Basses-  
1285 Terres du Saint-Laurent — Partie 2: Interprétation géologique. Ministère des Ressources  
1286 naturelles et de la Faune, Québec, DV 2012-04, 80 pp.

1287 Vengosh, A., R. B. Jackson, N. Warner, T. H. Darrah, Kondash, A. 2014. A critical review  
1288 of the risks to water resources from unconventional shale gas development and hydraulic  
1289 fracturing in the United States: *Environmental Science and Technology*, v. 48 no. 15, p.  
1290 8334-8348, doi: 10.1021/es405118y.

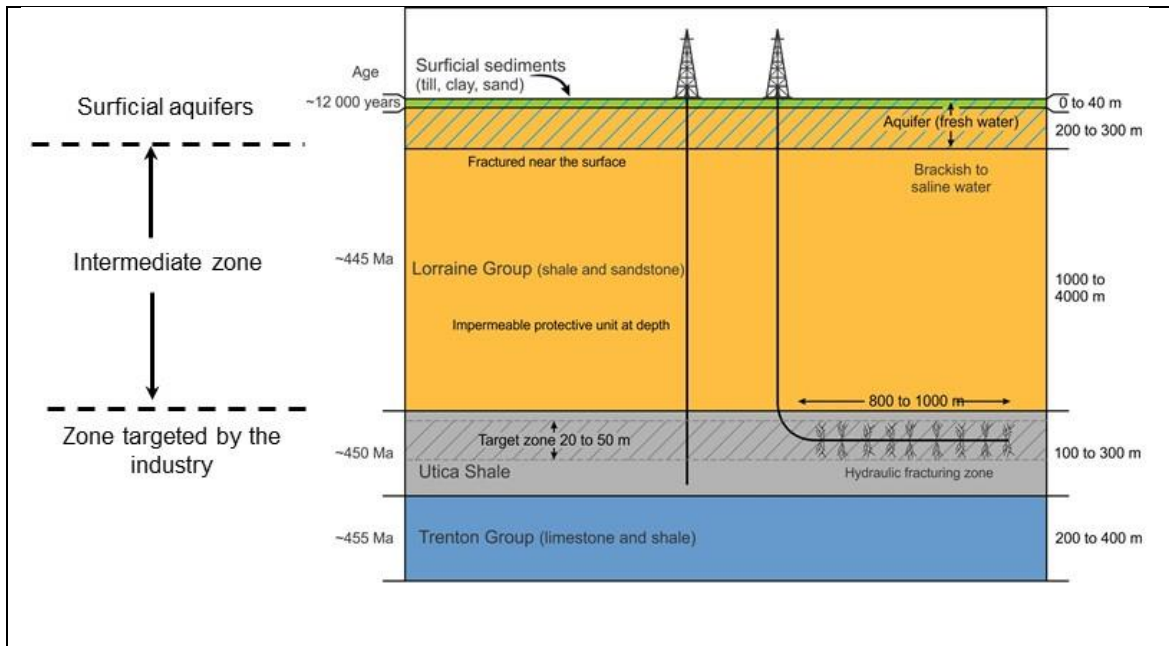
1291 Vidic, R.D., Brantley, S.L., Vandenbossche, J.M., Yoxtheimer, D., Abad, J.D. 2013.  
1292 Impact of shale gas development on regional water quality. *Science*, 340.

1293 Wang, Q., Gale, J.F. 2016. Characterizing Bedding-Parallel Fractures in Shale: Aperture-  
1294 Size Distributions and Spatial Organization. AAPG Annual Convention and Exhibition,  
1295 (Calgary, Alberta, Canada, June 22, 2016).

1296 Warner, N.R., Jackson, R.B., Darrah, T.H., Osborn, S.G., Down, A., Zhao, K., White, A,  
1297 Vengosh, A. 2012. Geochemical evidence for possible natural migration of Marcellus  
1298 Formation brine to shallow aquifers in Pennsylvania, vol. 109 no. 30, 11961–11966, doi:  
1299 10.1073/pnas.1121181109.

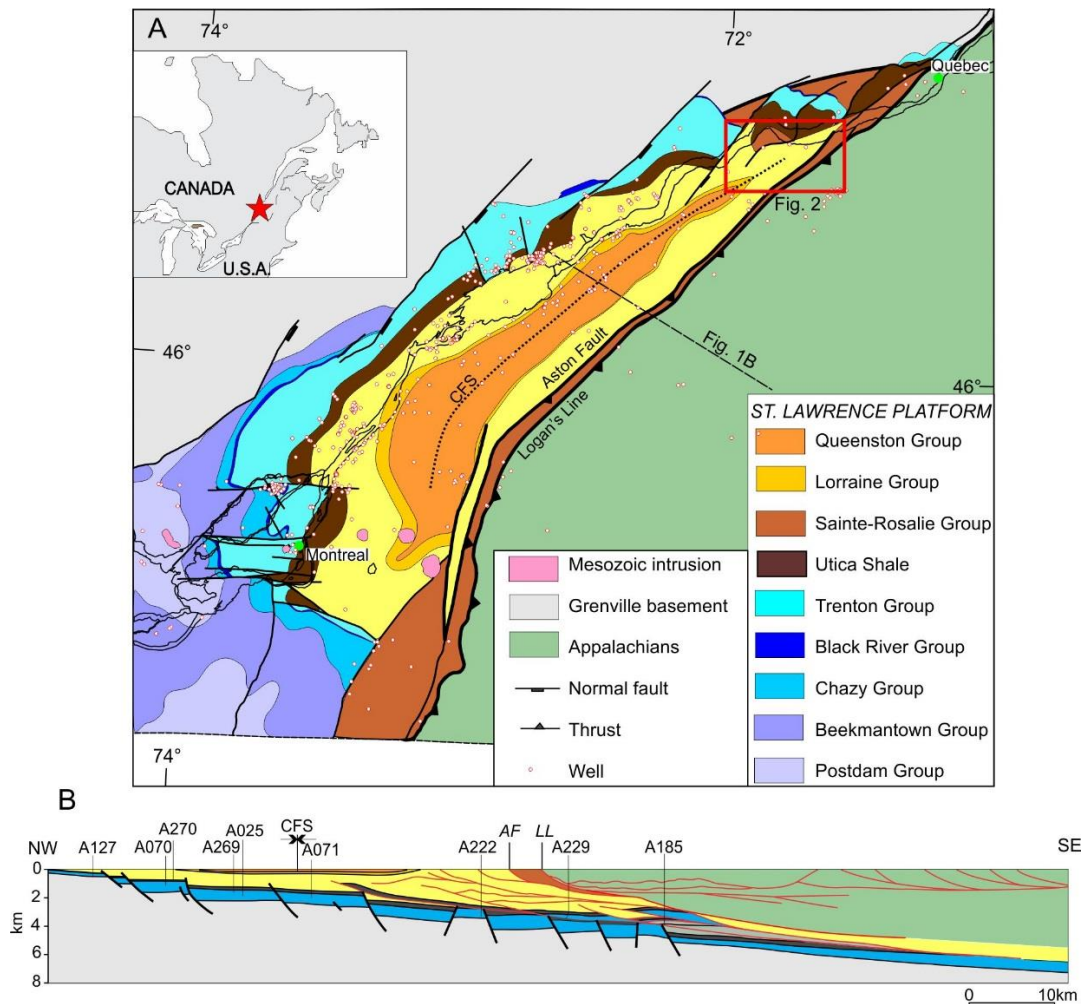
1300 Whiticar, M. J. 1999. Carbon and hydrogen isotope systematics of bacterial formation  
1301 and oxidation of methane. *Chemical Geology*, 161, 291–314.

1302



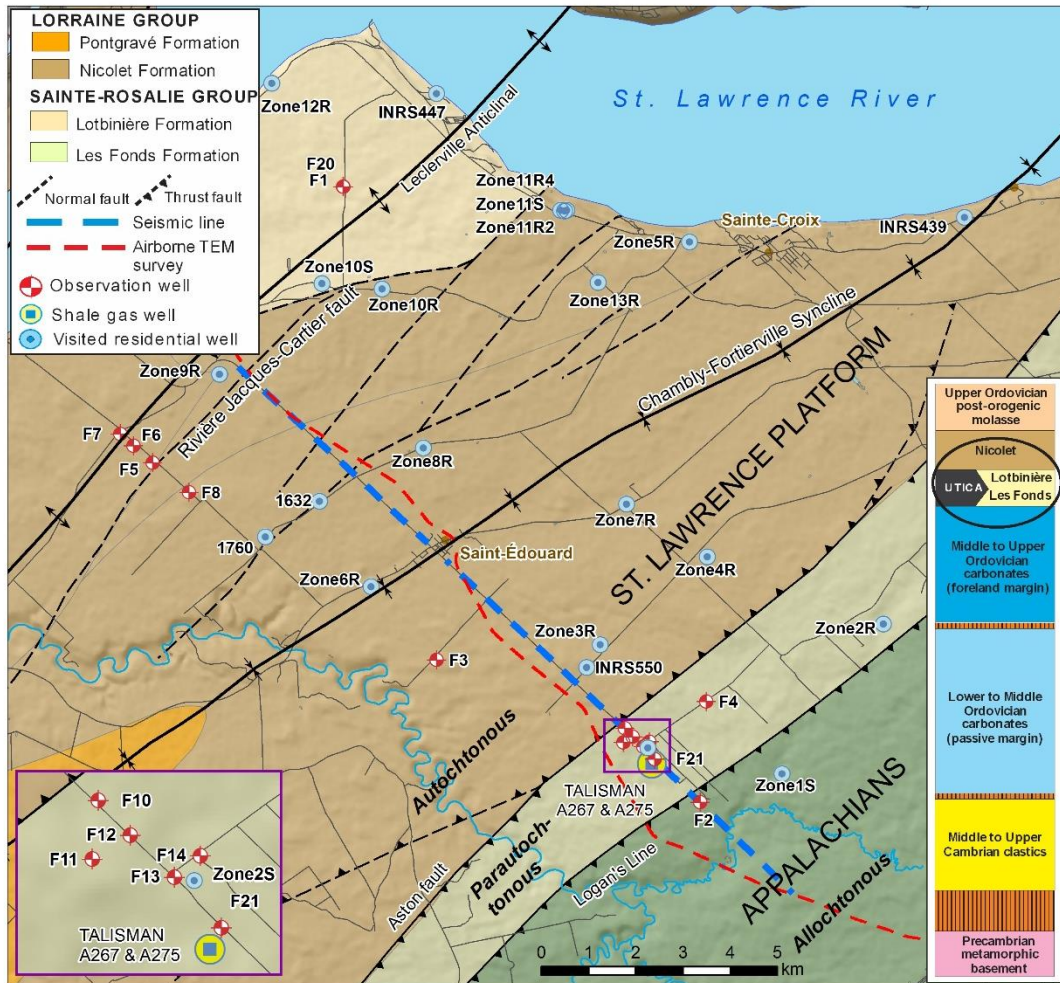
1303 Figure 1. Schematic geological cross-section presenting the different zones referred to in  
1304 this paper: shallow aquifers, intermediate zone and shale gas reservoir (in this case: the  
1305 Utica Shale).

1306



1307

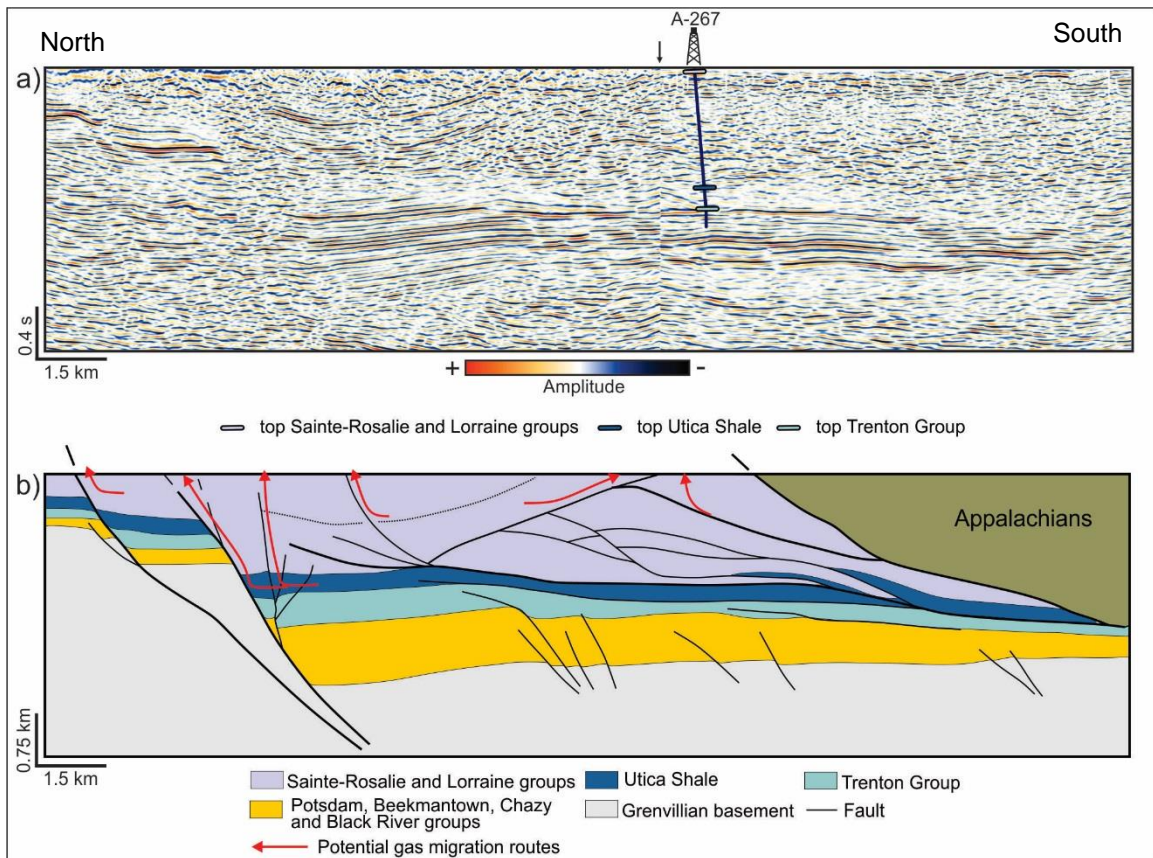
1308 Figure 2. A) Geological map of the St. Lawrence Platform between Montreal and Quebec  
 1309 City, southern Quebec, Canada (modified from Globensky, 1987). The Saint-Édouard  
 1310 study area is shown with a red box. B) Cross-section presenting the general  
 1311 tectonostratigraphic framework (modified from Séjourné et al., 2013). CFS: Chambly-  
 1312 Fortierville Syncline; AF: Aston Fault; LL: Logan's Line.



1313

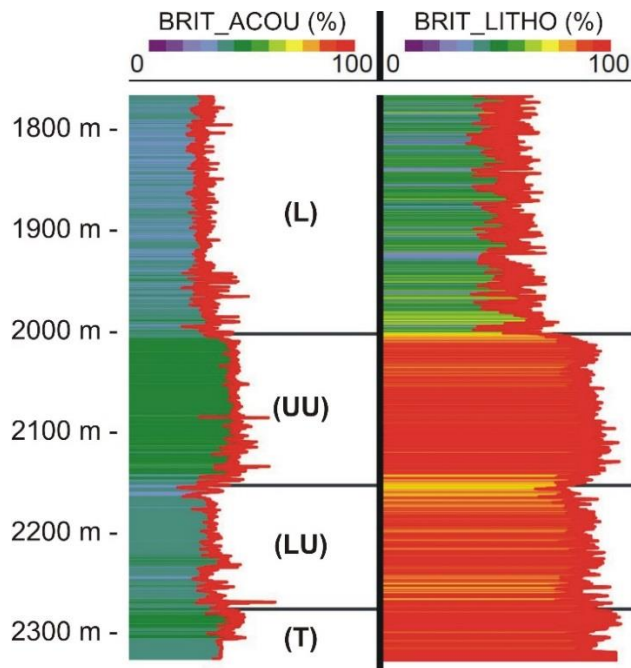
1314 Figure 3. Location of the Saint-Édouard area (red box on Figure 2) and of the observation  
 1315 and residential wells, along with the stratigraphic column (adapted from Rivard et al.,  
 1316 2018b).

1317



1318

1319 Figure 4. a) Uninterpreted industry seismic section crossing the Saint-Édouard wells (A-  
 1320 267 is the horizontal well) and b) geological interpretation of the seismic section shown in  
 1321 a) (modified from Lavoie et al., 2016). The arrow (at the top of the section on a) points at  
 1322 the location where two adjacent survey lines were merged together.

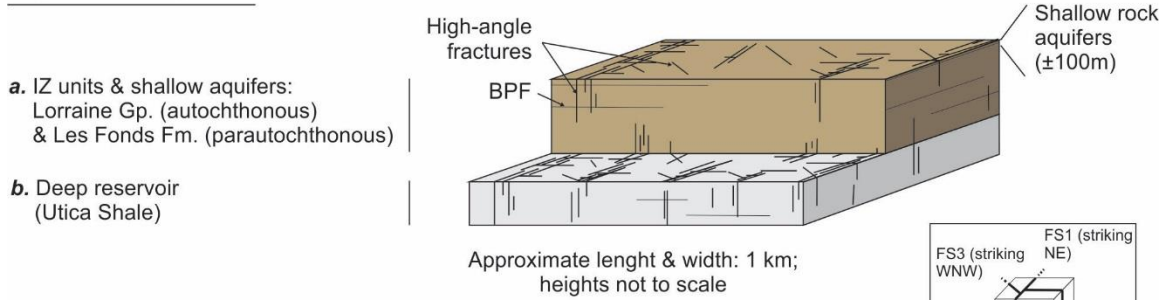


1323

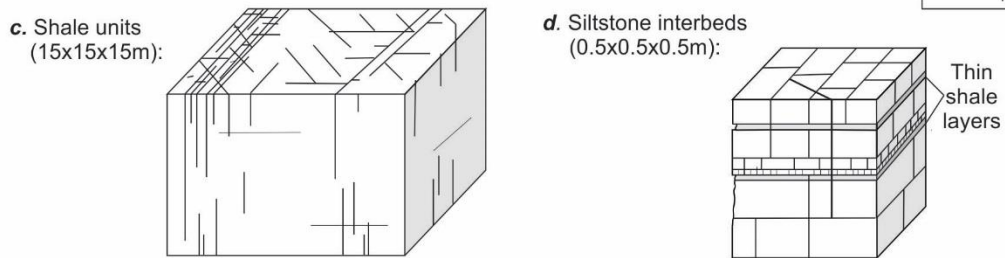
1324 Figure 5. Geomechanical profile of the lower section of the Fortierville shale gas well  
 1325 illustrating the vertical variations in the acoustic brittleness index (BRIT\_ACOU) and the  
 1326 mineralogical brittleness index (BRIT\_LITHO) across the base of the Lorraine Groupe (L),  
 1327 the upper and the lower parts of the Utica Shale (respectively UU and LU) and limestones  
 1328 at the top of the Trenton Group (T). The higher the value of the index, the more brittle is  
 1329 the strata. Note that the two independently calculated indexes display similar trends, but  
 1330 with different absolute values, which is explained by the different nature of the physical  
 1331 properties considered (acoustic versus mineralogic). Modified from Séjourné (2017).

1332

Regional fracture pattern



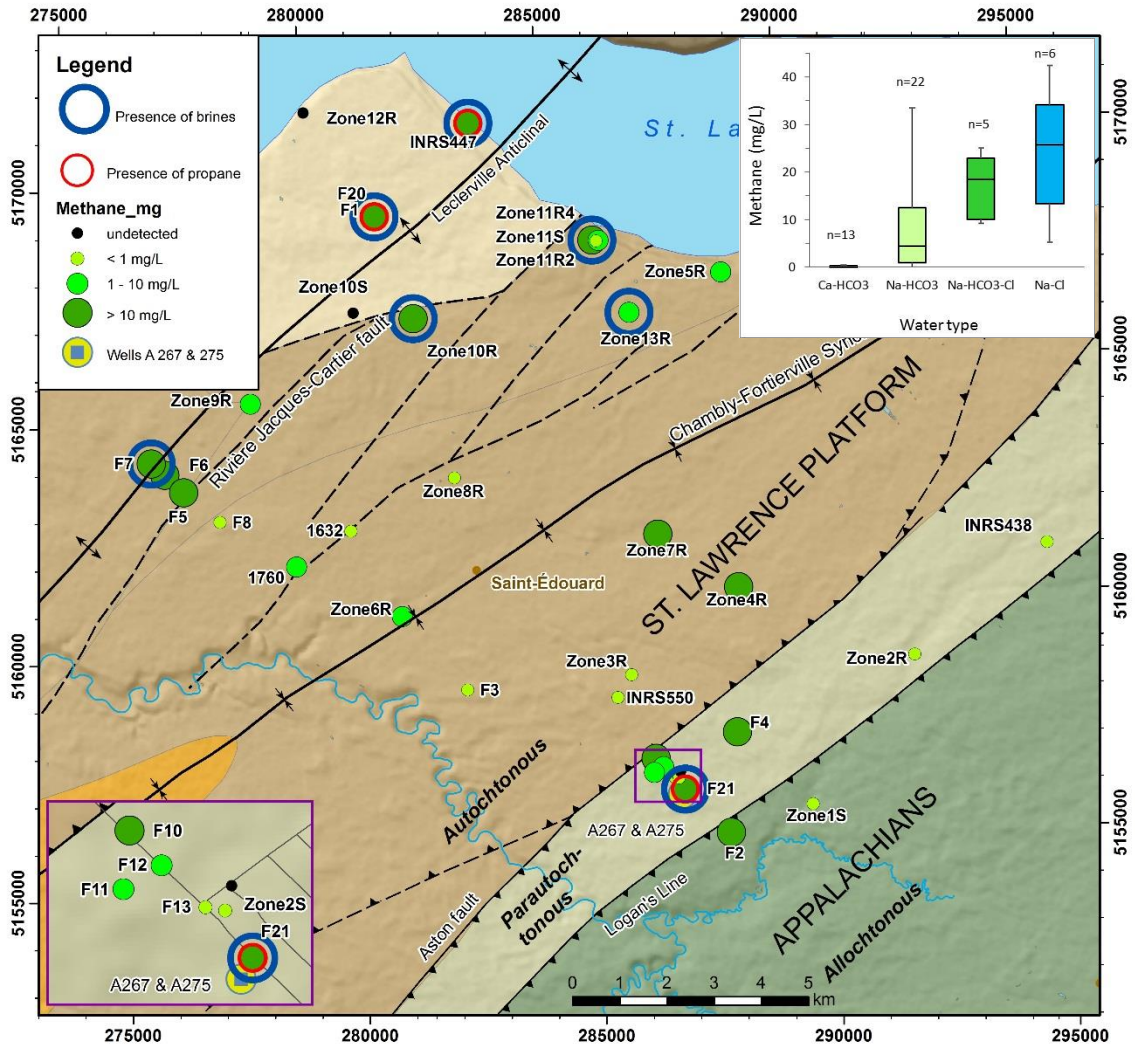
Representative Elementary Volumes (REV)



1333

1334 Figure 6. Conceptual models of the fracture network (modified from Ladevèze et al.,  
 1335 2018b). The regional fracture pattern is represented in **a.** for the shallow aquifers and  
 1336 intermediate zone (IZ) units; in **b.** for the deep reservoir. The fracture pattern is also  
 1337 represented using representative elementary volumes (REV) at a much more local scale  
 1338 for: **c.** shale units and **d.** siltstone interbeds. BPF: Bedding parallel fracture.

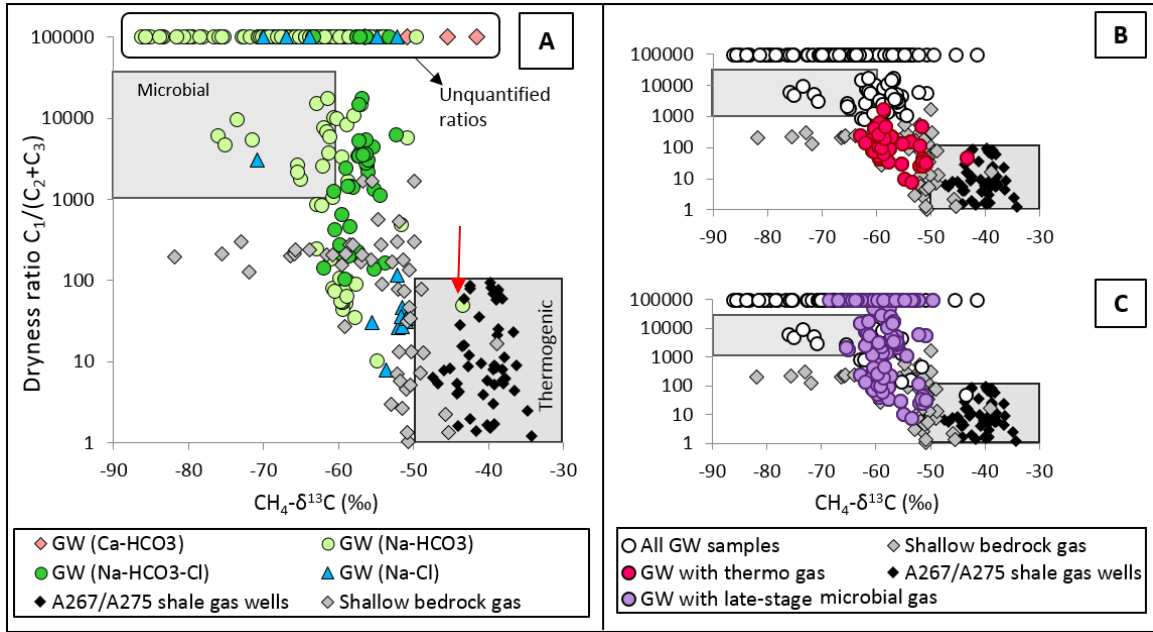
1339



1340

1341 Figure 7. Spatial distribution of dissolved methane concentrations. Bedrock geology  
 1342 legend as in Figure 3. Inset: boxplot of methane concentrations as a function of water  
 1343 type.

1344



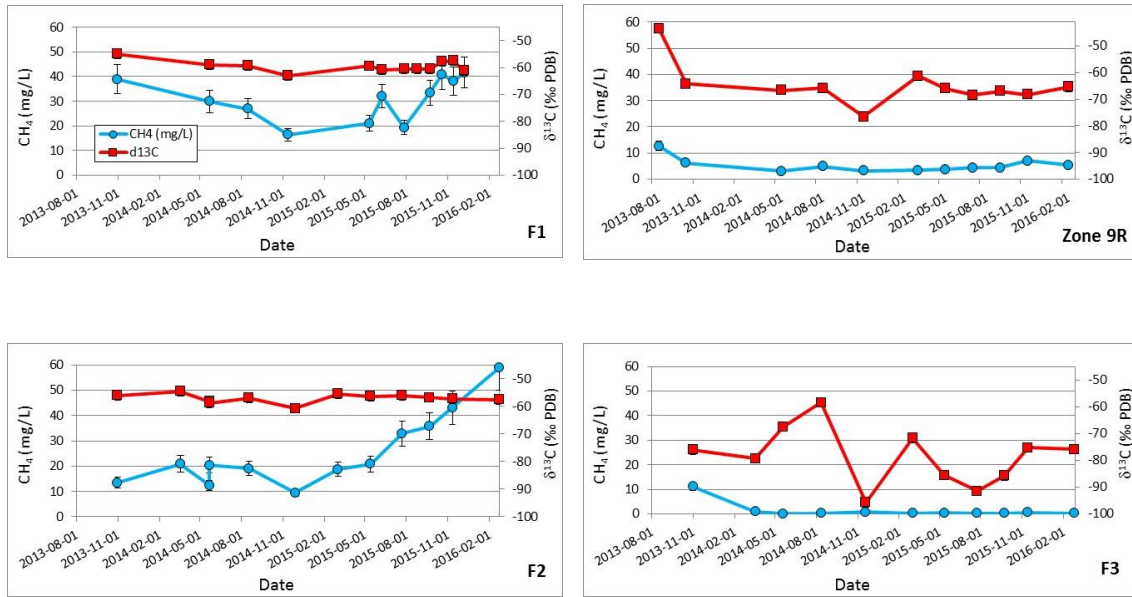
1345

1346 Figure 8. Bernard graphs showing the dryness ratio versus methane carbon isotopic  
 1347 composition obtained from shallow groundwater, shallow bedrock gas samples, and deep  
 1348 formation gas data published by Chatellier et al. (2013). A) Groundwater samples are  
 1349 classified according to their water type; B) emphasis on groundwater samples containing  
 1350 thermogenic gas and C) on groundwater samples containing late-stage microbial gas or  
 1351 microbial gas affected by oxidation (bottom). Gray boxes represent typical microbial and  
 1352 thermogenic gas domains.

1353

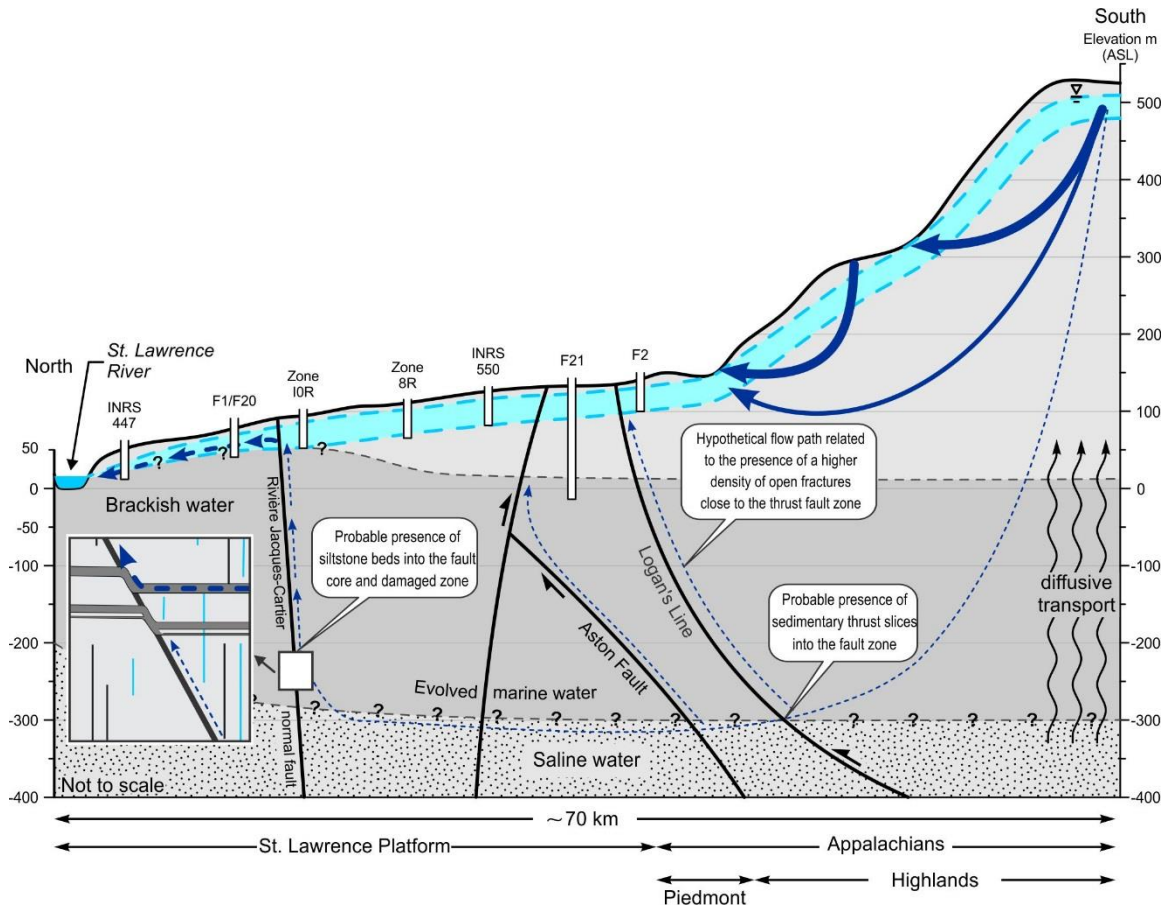
1354

1355



1356 Figure 9. Examples of dissolved methane concentrations over time for four of the seven  
 1357 observation wells (blue), along with the methane carbon isotopic ( $\delta^{13}\text{C}$ ) values (red).  
 1358 Uncertainty, represented by error bars, is  $\pm 15\%$  of the values for concentrations and  $1.7\%$   
 1359 for  $\delta^{13}\text{C}$  (nearly impossible to see) (estimated in Rivard et al., 2018a).

1360



1361

1362 Figure 10. Conceptual model of the regional groundwater flow. Modified from Bordeleau  
 1363 et al. (2018a) and Ladevèze et al. (2018b). Groundwater flow is indicated using blue arrows  
 1364 whose size is related to the relative magnitude of groundwater flow.

1365

1366

1367 **Supplementary information**

1368

1369 **Additional work that proved less conclusive**

1370

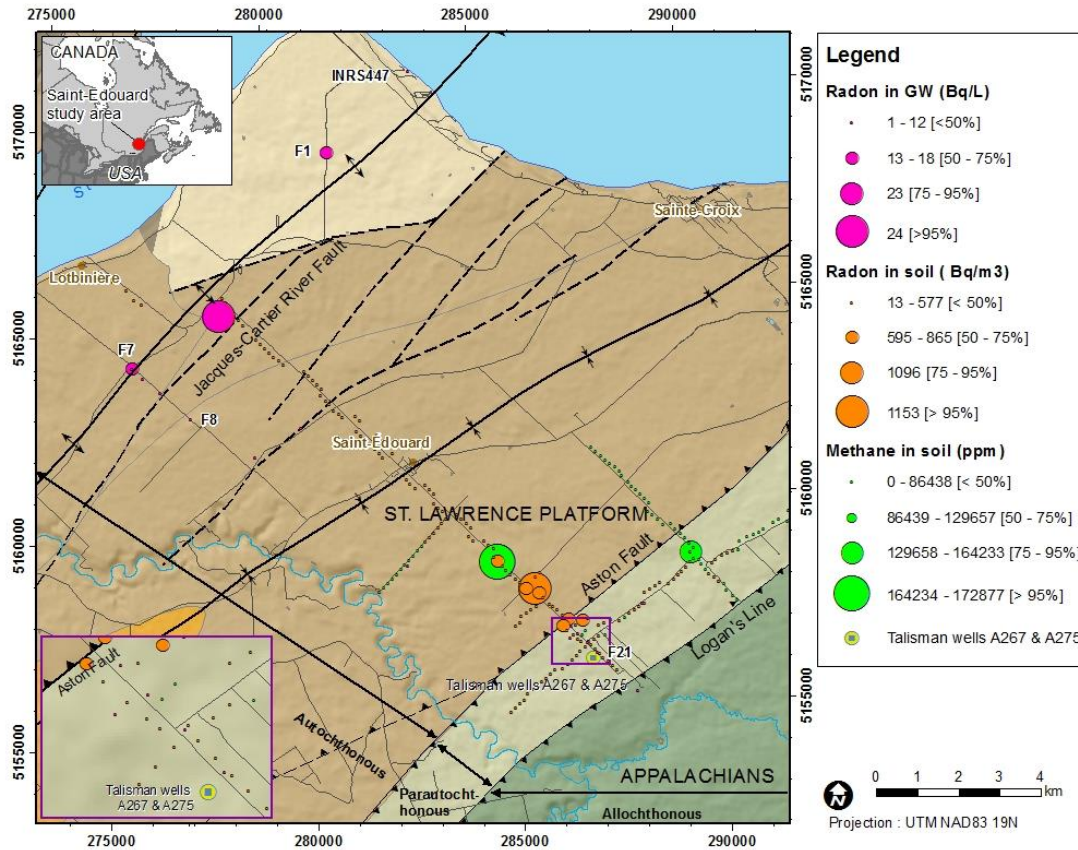
1371 Other analyses and fieldwork than those presented in the paper were attempted during the  
1372 course of the project, but led to results that were not as useful as expected. Although this  
1373 often occurs in research projects, as this paper is meant to provide an overview of the  
1374 multidisciplinary work and multi-source data collection that was undertaken, it was  
1375 decided to briefly present some of this work in this section. Nonetheless, these activities  
1376 could be successful and beneficial in other contexts. The main activity that did not reach  
1377 its objective is the shallow high resolution seismic survey that aimed to image the upper  
1378 portion of the intermediate zone, especially in fault zones. However, this activity was  
1379 discussed in section 3 and will not be addressed here.

1380

1381 *Soil gas geochemistry*

1382 A survey of soil gas concentrations (CO<sub>2</sub>, radon, methane, ethane, propane, butane) was  
1383 planned early in the project to try to indirectly identify areas containing more hydrocarbons  
1384 and radon in soils, which could have implied that upward fluid migration was actively  
1385 occurring in the study area. The soil hydrocarbon gas survey was carried out over 247  
1386 stations, whereas radon gas was measured at 155 stations (Aznar and Malo, 2014).

1387 Methane was found to be very abundant locally in soils, especially in the southeastern part  
1388 of the study area. However, locations with high methane concentrations were neither  
1389 correlated with locations having high ethane, propane and butane concentrations in soil  
1390 gas, nor with high methane concentrations in groundwater. Therefore, it is believed that  
1391 the major part of methane in soil gas is produced locally by microorganisms at shallow  
1392 depths, and is not an indication of higher concentrations at somewhat greater depths in the  
1393 bedrock aquifer. The highest concentrations of radon in soils were also detected in the  
1394 southeastern part of the surveyed area, and do not correspond to the locations of higher  
1395 radon concentrations in groundwater (Figure S1). However, it is interesting to note that the  
1396 highest radon concentrations in groundwater were found along the normal fault (F7, Zone  
1397 9R) and to the north of it (F1), where presence of small amounts of deep formation brines  
1398 was inferred from geochemical data. Unfortunately, no soil gas samples were collected in  
1399 the vicinity of wells Zone 9R, F7 and F1.



1400

1401 Figure S1. Spatial distribution of methane and radon ( $^{222}\text{Rn}$ ) in soil, as well as radon

1402 ( $^{222}\text{Rn}$ ) in groundwater of the Saint-Édouard area, using different percentile classes.

1403 Uranium values in rock represent mean values for the different sampled depths.

1404

1405 *HTEM survey*

1406 Since the shallow seismic survey could not help locate the surface extension of known fault

1407 zones, a 75 km-long helicopter-borne transient electromagnetic (HTEM) survey was flown,

1408 from a topographic high in the Appalachians to the St. Lawrence River. The helicopter

1409 flew at a mean altitude of 109 m above the ground with an average survey speed of 80

1410 km/h. This survey was designed to locate fault zones and map out the freshwater-saltwater  
1411 interface. Information on the depth of saline water is important, as it is much denser than  
1412 freshwater and, hence, plays an important role in the system hydrodynamics.

1413 The interpretation was carried out in a two-step procedure. First, a classical 1-D layered  
1414 inversion using seven layers based on data from resistivity logs (see section 5.2) was used,  
1415 but it did not provide results that seemed to fit with the current knowledge of the study  
1416 area, particularly in the vicinity of the RJC fault. Second, HTEM data were inverted using  
1417 laterally constrains (Auken et al., 2005) and Bayesian inversion using non-stationary  
1418 Matérn matrix (Bouchedda et al., 2017). This allowed for a more laterally continuous and  
1419 more accurate spatial distribution of the electrical resistivity of the ground. The second  
1420 resistivity model tended to confirm that there is a compartmentalisation of groundwater  
1421 flow on each side of the normal fault zone. Resistivity contrasts in the vicinity of the fault  
1422 zone indeed suggest that the latter could constitute a barrier to flow, especially around the  
1423 normal RJC fault. Evidence of such compartmentalisation has been provided by  
1424 geochemical data (see section 6.1).

1425

#### 1426 *Geomechanical laboratory testing*

1427 Laboratory tests on core samples had been planned to calibrate the geomechanical  
1428 parameters derived from acoustic and other petrophysical logs from shale gas wells.  
1429 However, the only deep shale core samples that were available for physical testing  
1430 consisted of one quarter of a 2.5 inches cores, which were, moreover, very friable.  
1431 Therefore, it had been decided to strengthen these samples with a cement grout or gypsum

1432 that had similar geomechanical properties than this shale to run dynamic (acoustic) tests  
1433 and static (uni- and tri-axial compression) tests in laboratory.

1434 Results of the laboratory (dynamic) tests on these hybrid samples showed that most  
1435 Poisson's ratios had values outside the plausible range (0-0.5) and thus had to be rejected,  
1436 while the comparison for Young's modulus values with those obtained with well logs  
1437 showed that laboratory test values were significantly lower. These low values are likely  
1438 due to a loss of structural integrity of the core samples, which could have occurred during  
1439 their *in situ* sampling, transport or handling in the laboratory or could be due to the  
1440 inadequacy of cementation for these samples. It was thus concluded that these grouted core  
1441 samples could not provide reliable values in this case. These laboratory tests, their results  
1442 and comparison with those obtained from well logs are discussed in Séjourné (2016).

1443

#### 1444 *Downhole gas sensors*

1445 Efforts were also invested in downhole sensors for monitoring purposes, as it had been  
1446 observed early in the project that methane concentrations could vary significantly over time  
1447 in this region and it would have been interesting to have more information about short-term  
1448 (at least daily) variations. Two types of sensors were installed in a few observation wells:  
1449 the first type provided total dissolved gas pressure (TDGP), while the second type  
1450 measured both TDGP and methane. TDGP sensors were meant to provide a proxy for  
1451 dissolved methane concentrations, as methane is difficult to estimate using permeable  
1452 membranes when concentrations are significant (above 1 mg/L with the probes that were

1453 used for this project). Downhole gas sensors were deployed in three wells to measure daily  
1454 methane concentrations in groundwater.

1455 The TDGP sensors did not provide reliable values, as groundwater in these wells is  
1456 effervescent and is thus degassing; hence dissolved gas could escape through the free phase  
1457 as the sensors had not been installed below a packer. Moreover, chemical analysis of the  
1458 different dissolved gases (N<sub>2</sub>, CO<sub>2</sub>, O<sub>2</sub>+Ar, and C<sub>1</sub>-C<sub>5</sub> alkanes) over time in the selected  
1459 wells showed that the proportions of individual gases may vary significantly; hence, TDGP  
1460 is not a good proxy for methane concentrations in this region.

1461 The methane sensor did not generate useful data because methane concentrations were  
1462 quite high and as the permeable membrane inside becomes saturated, it takes several days,  
1463 even weeks, to adapt to new conditions. Although downhole sensors appear to be promising  
1464 tools for methane monitoring, additional technical development must be performed before  
1465 they can be routinely used in a gas-rich environment.

1466

#### 1467 *Strontium isotopes*

1468 Stable strontium isotopic ratios (<sup>87</sup>Sr/<sup>86</sup>Sr) were analysed in 23 groundwater samples, seven  
1469 (7) shallow bedrock (41-146 m) samples, and three (3) deep rock samples from the Lorraine  
1470 (1745 m) and Utica (1883 and 2000 m) shales. These analyses were planned because  
1471 strontium has proven to be a useful tracer for groundwater flow paths (Clark and Fritz,  
1472 1997).

1473  $^{87}\text{Sr}/^{86}\text{Sr}$  ratios varied widely, ranging from 0.7091 to 0.7151 in groundwater and from  
1474 0.7085 to 0.7313 in rock samples. The  $^{87}\text{Sr}/^{86}\text{Sr}$  ratios in groundwater follow the trends of  
1475 their respective host rock formation, but with less radiogenic values, indicating that the  
1476 isotopic signature of the shallow rock formations is imparted to the groundwater, along  
1477 with another, less radiogenic Sr end-member. Potential candidates for this end-member  
1478 include Utica Shale brines, Champlain Sea water, or overburden sediments. Brines from  
1479 the intermediate zone are another potential candidate, but no data is available for rocks  
1480 between 146 m and 1745 m. The measured  $^{87}\text{Sr}/^{86}\text{Sr}$  ratios did not allow identifying the  
1481 end-member, but mass balance calculations considering Sr concentrations advocate against  
1482 Utica Shale brines. Hence, Sr isotopic analyses did not provide exclusive information and  
1483 did not unequivocally allow ruling out the presence of Utica brines in shallow groundwater,  
1484 but the results are still consistent with our interpretation of the hydrogeological system in  
1485 this area (Bordeleau et al., 2018).

1486

1487 *Pore-water from shallow and deep shale samples*

1488 As an upward flow of formation brines was identified in the vicinity of the RJC normal  
1489 fault but the depth of the source is unknown, an attempt was made at analysing pore water  
1490 in shale core samples from shallow (0-150 m) and deep (1900- 2500 m) wells, based on  
1491 the work of Clark et al. (2013). The rationale was that some brine might still be trapped in  
1492 the pore space of the rock samples, and its geochemical fingerprint could be compared to  
1493 the brines found in groundwater (similar to what was done with the shallow bedrock  
1494 alkanes and groundwater alkanes). Unfortunately, not enough pore-water could be

1495 extracted from these tight shale samples, and analyses of Br/Cl and  $^{87}\text{Sr}/^{86}\text{Sr}$  ratios could  
1496 not be performed.

1497

1498 *Presence of phospholipid fatty acids (PLFAs)*

1499 Analyses of phospholipid fatty acids (PLFAs) from crushed shale samples from the  
1500 Nicolet, Lotbinière and Les Fonds formations were attempted in order to identify  
1501 biomarkers for *in situ* active microbial population. Distributions and stable carbon isotope  
1502 ratios ( $\delta^{13}\text{C}$ ) of PLFAs can provide valuable insight into sources and biogeochemical  
1503 cycling of carbon (Ahad and Pakdel, 2013). However, despite repeated attempts to extract  
1504 PLFAs using large amounts of crushed rock (between 0.5 to 1.0 kg), PLFA yields from  
1505 these samples were consistently around the same trace levels as those determined in process  
1506 blanks. Although no direct understanding into microbial carbon sources could be obtained,  
1507 these results indicate very little active microbial carbon cycling within the shale, and thus  
1508 point to an ancient or pre-existing source of methane in groundwater samples not associated  
1509 with on-going microbial utilization of fossil carbon. Therefore, late-stage methanogenesis  
1510 that was recognized in a large number of groundwater samples in this study area would  
1511 likely be attributable to old methane generated in the distant geological past, and not recent  
1512 methane produced by microbes using old carbon.

1513

1514

1515

1516 *Presence of naphthenic acids (NAs)*

1517 Acid extractable organics (AEOs) in groundwater samples were analysed to determine the  
1518 occurrences, distributions and sources of naphthenic acids (NAs) in the subsurface (Ahad  
1519 et al., 2018). As classically defined by  $C_nH_{2n+Z}O_2$ , the most abundant NAs detected in the  
1520 majority of groundwater samples' AEOs were straight-chain ( $Z = 0$ ) or monounsaturated  
1521 ( $Z = -2$ )  $C_{16}$  and  $C_{18}$  fatty acids. Several groundwater samples, however, contained  
1522 significant proportions of potentially toxic alicyclic bicyclic NAs (i.e.,  $Z = -4$ ) in the  $C_{10}$ -  
1523  $C_{18}$  range. These compounds may have originated from migrated waters containing a  
1524 different distribution of NAs, or are the product of *in situ* microbial alteration of shale  
1525 organic matter and petroleum. Although concentrations of AEOs were very low ( $< 2.0$   
1526 mg/L), the detection of these compounds in groundwater overlying an undeveloped  
1527 unconventional hydrocarbon reservoir points to a natural background source. In light of  
1528 these findings, routine screening for NAs in environmental samples from areas undergoing  
1529 shale gas development may be warranted.

1530

1531 **References**

1532

1533 Ahad, J.M.E., Pakdel, H. 2013. Direct evaluation of in situ biodegradation in Athabasca  
1534 oil sands tailings ponds using natural abundance radiocarbon. *Environmental Science &*  
1535 *Technology* 47, 10214–10222.

1536 Ahad, J.M.E., Pakdel, H., Lavoie, D., Lefebvre, R., Peru, K.M. & Headley, J.V. 2018.  
1537 Naphthenic acids in groundwater overlying undeveloped shale gas and tight oil reservoirs.  
1538 *Chemosphere* 191, 664-672.

1539 Auken, E., A. V. Christiansen, B. H. Jacobsen, N. Foged, and K. I. Sørensen. 2005.  
1540 Piecewise 1D Laterally Constrained Inversion of resistivity data,  
1541 *Geophysical Prospecting*, 53, 497-506.

1542 Aznar, J.C. et Malo, M., 2014. Échantillonnage des gaz de sol dans la région de St.  
1543 Édouard, sud du Québec, Canada; Commission géologique du Canada, Dossier public  
1544 7729, 69 pages. doi:10.4095/295539.

1545 Bordeleau, G., Rivard, C., Lavoie, D., Lefebvre, D., Malet, X. 2018. Geochemical study of  
1546 the Saint-Édouard area, southern Quebec, Geological Survey of Canada, Open File,  
1547 submitted.

1548 Bouchedda, A., Giroux, B, Gloaguen, E. 2017. Constrained electrical resistivity  
1549 tomography Bayesian inversion using inverse Matérn covariance matrix. *Geophysics*,  
1550 82(3):E129-E141.DOI : 10.1190/geo2015-0673.1

1551 Clark, I. D., Al, T., Jensen, M., Kennell, L., Mazurek, M., Mohapatra, R., Raven, K. G.  
1552 (2013). Paleozoic-aged brine and authigenic helium preserved in an Ordovician shale  
1553 aquiclude. *Geology*, 41(9), 951-954.

1554 Clark, I.D., Fritz, P. 1997. Environmental Isotopes in Hydrogeology. CRC Press, Boca  
1555 Raton, 185.Séjourné, S. 2016. Étude des données géomécaniques de laboratoire des  
1556 carottes d'un puits pétrolier et gazier (Talisman, Saint-Édouard No 1), région de Saint-

1557 Édouard, Québec; Commission géologique du Canada, Dossier public 7893, 2016; 54  
1558 pages, doi:10.4095/297780.



1560 **Supplementary tables**

1561

1562 Table S-1: Characteristics of the observation wells

Site	Drilling type	Drilling year	Total drilled depth (m)	Static water level (m below TOC)	Overburden thickness (m)	Sampling depth (m below TOC)	Conditions	K (m/s)	Geological formation
F1	Diamond	2013	50	1.86	2.44	7.5	Semi-confined	$5.93 \times 10^{-7}$	Lotbinière
F2	Diamond	2013	52	2.76	6.10	21.5	Semi-confined	$2.38 \times 10^{-7}$	Les Fonds
F3	Diamond	2013	50	1.68	20.12	22.7	Confined	$3.97 \times 10^{-7}$	Nicolet
F4	Diamond	2013	60	8.87	40.84	54.0	Confined	$3.02 \times 10^{-6}$	Les Fonds
F5	Hammer	2014	52	2.30	9.75	14.4	Confined	$4.55 \times 10^{-7}$	Nicolet
F6	Hammer	2014	52	2.35	6.71	10.0	Confined	$2.00 \times 10^{-6}$	Nicolet
F7	Diamond	2014	52	4.42	11.43	17.7	Semi-confined	$1.10 \times 10^{-5}$	Nicolet
F8	Diamond	2014	52	0.72	1.43	20.2	Confined	$3.12 \times 10^{-6}$	Nicolet

F10	Hammer	2014	30	3.84	15.85	23.8	Confined	$6.15 \times 10^{-7}$	Les Fonds
F11	Hammer	2014	55	2.60	6.4	10.3	Semi-confined	$4.55 \times 10^{-8}$	Les Fonds
F12	Hammer	2014	73	3.02	7.92	20.4	Confined	$1.94 \times 10^{-7}$	Les Fonds
F13	Hammer	2014	61	2.13	1.83	7.7	Confined	$3.38 \times 10^{-9}$	Les Fonds
F14	Hammer	2014	30	30.92	14.33	dry	Confined	$5.78 \times 10^{-7}$	Les Fonds
F20	Diamond	2014	50	0.73	3.05	7.4	Semi-confined	$2.26 \times 10^{-9}$	Lotbinière
F21	Diamond	2014	147	3.60	3.05	145	Confined	$5.93 \times 10^{-7}$	Les Fonds

1563

1564 Notes:

1565 1) Diamond: Diamond-drilled well with a 100 mm (4 in.) diameter; Hammer: Hammer-drilled well with a 152 mm (6 in.) diameter. TOC: top of casing.

1566 2) During the 2013 drilling campaign, it was observed that pores in the shallow bedrock contained a lot of gas with the light components ( $C_1$  to  $C_3$ ) being mostly  
1567 lost due to evaporative loss. Therefore, core samples from the 2014 drilling program were carefully preserved for different types of hydrocarbon analyses (see  
1568 section 6.2). As the 2013 well F1 cores contained a significant volume of gas (but the light fraction was lost), well F20 was drilled next to it (6 m away) in  
1569 2014 to obtain data on the full spectrum of gas in the rock pores.

1570

Table S-2: Information or evidence for or against upward migration

<b>Discipline</b>	<b>Evidence in favor of potential large-scale upward migration</b>	<b>Evidence against large-scale upward migration</b>
Geophysics: seismic reflection and VTEM surveys	<p>Reprocessing and re-interpretation of deep old seismic surveys from the industry showed possibilities for upward migration to a certain depth. However, a clear reflector imaging in the upper ~1000 m of this survey was difficult and the near-surface seismic survey could not fill the gap due to the geological context that was not well suited for this method.</p> <p>The stochastic inversion of the VTEM survey revealed an anomalous feature that supports the assumption that the normal fault acts as a regional discharge zone by showing a drastic difference in saline water depths upstream and downstream of it.</p>	
Geomechanics		Based on geomechanical properties such as Poisson's coefficient and Young's modulus, the IZ was found to represent an efficient barrier to the propagation of induced fractures during hydraulic fracturing, thus providing a good protection for the shallow GW aquifers.

<p>Structural geology, borehole logging</p>	<p>Well-known regional fault zones are present in the study area: a normal fault zone in the northern part and a thrust – back-thrust fault system in the southern part.</p> <p>Data from deep shale gas wells showed that denser natural fracture networks can develop in the close vicinity of thrust faults.</p> <p>The presence of siltstone interbeds, which are more permeable than shale beds, have probably been dragged into the normal fault core in the upper part of the IZ, where they are frequently present. This would explain the presence of brines in shallow observation wells near the normal fault (see below).</p>	<p>The Utica Shale is known to be overpressured. This suggests that there is no “leak” from the gas reservoir.</p> <p>Density of the open natural fractures is very low at depth and the risk of connectivity is minimal.</p> <p>Open fractures at depth close to thrust faults are mostly parallel (in the same direction as fractures from FS1), greatly limiting possible interconnections and thus an increase in permeability.</p> <p>The IZ is composed of low <i>K</i> shale. This shale is clayey.</p> <p>Gouge is present in fault cores.</p>
<p>Hydrogeology</p>	<p>Although very few local data are available on the vertical hydraulic gradient, as the Utica Shale is overpressured, the overall gradient could make groundwater flow upward given that conditions (sufficient permeability and gradient) would allow it and counteract the opposite effect of high salinity on formation water density.</p>	<p>The presence of overpressure suggests that conditions for significant upward movement do not exist.</p>

<p>Geochemistry: groundwater, rocks, soils and GW monitoring</p>	<p>15% of the wells show a thermogenic component in groundwater.</p> <p>Presence of thermogenic gas and radon in soils.</p> <p>Groundwater geochemistry, and in particular geochemical profiles, showed that brines were present in a few shallow wells, mainly located close to or in the damage zone of the hanging wall of the normal fault. These brines with a higher Br/Cl ratio than sea water can only come from deeper units.</p> <p>Dissolved methane show very high fluctuations of methane concentrations, both spatially and temporally. Likewise, methane isotopic composition can show large variations over time.</p>	<p>Thermogenic methane found in GW does not have the same isotopic composition as methane in the Utica Shale.</p> <p>There is not more thermogenic methane in wells containing brines, indicating that the latter does not come from the Utica Shale.</p> <p>Both microbial and thermogenic gas appears to come from the shallow bedrock itself based on a comparison with gas extracted from shallow core samples.</p>
--	---	---

1572 Note: IZ: intermediate zone; GW: groundwater

1573